AGU PUBLICATIONS

Water Resources Research

RESEARCH ARTICLE

10.1002/2014WR015809

Key Points:

- Recharge ratios are highest during the winter in arid and temperate climates
- Recharge ratios are at a maximum during the wet season in the tropics
- Groundwater $\delta^{18}O$ and $\delta^{2}H$ values are often lower than annual precipitation

Supporting Information:

- Readme
- Supplementary information

Correspondence to:
S. Jasechko,
sjasechk@ucalgary.ca

Citation:
Jasechko, S., S. J. Birks, T. Gleeson, Y. Wada, P. J. Fawcett, Z. D. Sharp, J. J. McDonnell, and J. M. Welker (2014), The pronounced seasonality of global groundwater recharge, *Water Resour. Res.*, *50*, 8845–8867, doi:10.1002/2014WR015809.

Received 12 MAY 2014
Accepted 12 OCT 2014
Accepted article online 16 OCT 2014
Published online 18 NOV 2014

The pronounced seasonality of global groundwater recharge

Scott Jasechko[1,2], S. Jean Birks[3], Tom Gleeson[4], Yoshihide Wada[5], Peter J. Fawcett[1], Zachary D. Sharp[1], Jeffrey J. McDonnell[6,7], and Jeffrey M. Welker[8]

[1]Department of Earth and Planetary Sciences, University of New Mexico, Albuquerque, New Mexico, USA, [2]Department of Geography, University of Calgary, Calgary, Alberta, Canada, [3]Alberta Innovates—Technology Futures, Calgary, Alberta, Canada, [4]Department of Civil Engineering, McGill University, Montreal, Quebec, Canada, [5]Department of Physical Geography, Faculty of Geosciences, Utrecht University, Utrecht, Netherlands, [6]Global Institute for Water Security, University of Saskatchewan, Saskatoon, Canada, [7]School of Geosciences, University of Aberdeen, Aberdeen, Scotland, UK, [8]Department of Biological Sciences, University of Alaska Anchorage, Anchorage, Alaska, USA

Abstract Groundwater recharged by meteoric water supports human life by providing two billion people with drinking water and by supplying 40% of cropland irrigation. While annual groundwater recharge rates are reported in many studies, fewer studies have explicitly quantified intra-annual (i.e., seasonal) differences in groundwater recharge. Understanding seasonal differences in the fraction of precipitation that recharges aquifers is important for predicting annual recharge groundwater rates under changing seasonal precipitation and evapotranspiration regimes in a warming climate, for accurately interpreting isotopic proxies in paleoclimate records, and for understanding linkages between ecosystem productivity and groundwater recharge. Here we determine seasonal differences in the groundwater recharge ratio, defined here as the ratio of groundwater recharge to precipitation, at 54 globally distributed locations on the basis of $^{18}O/^{16}O$ and $^{2}H/^{1}H$ ratios in precipitation and groundwater. Our analysis shows that arid and temperate climates have wintertime groundwater recharge ratios that are consistently higher than summertime groundwater recharge ratios, while tropical groundwater recharge ratios are at a maximum during the wet season. The isotope-based recharge ratio seasonality is consistent with monthly outputs from a global hydrological model (PCR-GLOBWB) for most, but not all locations. The pronounced seasonality in groundwater recharge ratios shown in this study signifies that, from the point of view of predicting future groundwater recharge rates, a unit change in winter (temperate and arid regions) or wet season (tropics) precipitation will result in a greater change to the annual groundwater recharge rate than the same unit change to summer or dry season precipitation.

1. Introduction

Groundwater resources support one third of human water use [*Wada et al.*, 2014] and represent ~99% of Earth's unfrozen fresh water [*Aeschbach-Hertig and Gleeson*, 2012]. Groundwater has inputs from the infiltration of water from the surface, and has losses via discharge to the surface (streams, springs, seeps, lakes, and ocean), terrestrial transpiration and evaporation and groundwater pumping. Groundwater provides two billion people with drinking water and supplies 40% of global cropland irrigation [*Siebert et al.*, 2010; *Foley et al.*, 2011]. In spite of groundwater's pivotal importance to human livelihood, current extractions are depleting certain aquifers at several times the nature rate of replenishment [*Konikow and Kendy*, 2005; *Wada et al.*, 2010; *Konikow*, 2011; *Gleeson et al.*, 2012]. Examples of nonsustainable groundwater use have been observed in multiple regions including the northern Gangetic Plain (India) [*Rodell et al.*, 2009], the North China Plain [*Feng et al.*, 2013], the Middle East [*Voss et al.*, 2013; *Joodaki et al.*, 2014], the High Plains (central United States) [*Scanlon et al.*, 2012; *Steward et al.*, 2013], the Colorado River basin (southwest United States) [*Castle et al.*, 2014], and the Californian Central Valley (western United States) [*Famiglietti et al.*, 2011; *Scanlon et al.*, 2012]. The reversal of current nonsustainable groundwater extraction rates will require setting long-term pumping rate goals that will achieve a balance with groundwater recharge and ecosystem groundwater requirements [*Gleeson et al.*, 2012; *Aeschbach-Hertig and Gleeson*, 2012]. To determine sustainable groundwater pumping rates requires accurate estimates of groundwater recharge rates and thorough understanding of seasonal controls upon recharge.

10.1002/2014WR015809

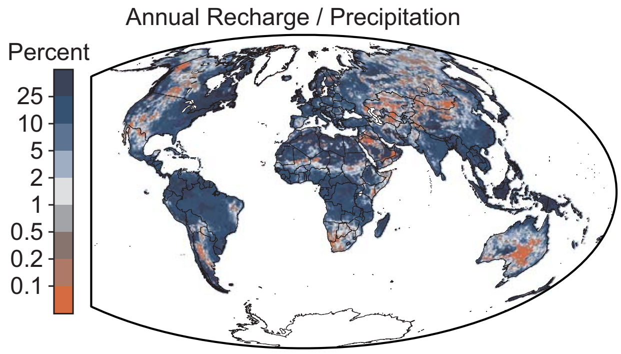

Figure 1. The global mean annual groundwater recharge ratio (i.e., recharge as a proportion of precipitation) calculated using a global hydrological model **(**PCR-GLOBWB**)** **[***Wada et al*., 2010].

Groundwater recharge is a complex ecohydrological process controlled by the physical state, amount and intensity of precipitation, and by the topography, water table level, geology, soil type, vegetation characteristics, boundary layer climatology, and irrigation return flows. Global syntheses of chloride mass balance recharge fluxes suggest that vegetation characteristics are the second most important determinant for groundwater recharge after precipitation fluxes [*Kim and Jackson*, 2012]. This is consistent with recent work showing that transpiration exceeds physical evaporation on continents [*Jasechko et al*., 2013]. While investigations of annual groundwater recharge are common [e.g., *Scanlon et al*., 2006; *Döll and Fielder*, 2008; *Wada et al*., 2010] and several have explored mechanistically the interaction of the various ecological and physical factors controlling recharge in different settings [e.g., *Pangle et al*., 2014; *Kurylyk et al*., 2014], few investigations have studied explicitly the seasonal distribution of groundwater recharge. Examining this seasonal distribution or intra-annual variability in groundwater recharge is important because human-induced climate change impacts the hydrology of each season differently [e.g., *Hayhoe et al*., 2004; *Vera et al*., 2006].

Here we examine the seasonality of recharge with the *groundwater recharge ratio*, defined herein as groundwater recharge as a proportion of precipitation (recharge/precipitation). Previous work has estimated the annual global groundwater recharge ratio using a hydrological model and found a global mean of $\sim$16% (PCR-GLOBWB) [*Wada et al*., 2010] (Figure 1). However, model estimates are highly uncertain as a result of sparse hydrogeological data and because of static land use representations in current models [e.g., *Döll and Fielder*, 2008; *Wada et al*., 2010]. Furthermore, projections of change to groundwater recharge from climate warming may neglect the importance of extreme events or changes to seasonal processes if based solely upon averages [*Portmann et al*., 2013].

Intuitively, groundwater recharge during spring snowmelt in higher latitudes should be the largest of the hydrological year given the multiweek concentrated input and lack of competing evapotranspiration demands on water inputs [*Dunne and Leopold*, 1978; *Clark and Fritz*, 1997]. In more arid regions, one would likewise expect intuitively that disproportionate amounts of groundwater recharge would occur during summer monsoon conditions or during periods of concentrated high intensity rainfall. Indeed, site-specific modeling and field-studies have shown many examples this is the case, with winter recharge ratios that are higher than summer recharge ratios in Belgium [*Leterme et al*., 2012], Greenland [*Leterme et al*., 2012], the northeastern United States [*Heppner et al*., 2007; *Yeh and Famiglietti*, 2009; *Dripps and Bradbury*, 2010; *Dripps*, 2012], and Croatia [*Jukić and Denić-Jukić*, 2009], and summer recharge that is restricted solely to high intensity thundershowers in some locations (e.g., Wisconsin, USA) [*Dripps*, 2012]. In terms of the groundwater recharge ratio, long-term monitoring of groundwater recharge in Tanzania, for instance, has shown that the recharge ratio is at a maximum during intense rain events [*Taylor et al*., 2013] and occurs almost exclusively during the wet season. Similarly, winter recharge in temperate climates has been found to be an extreme and rapid process during spring freshet [*Sklash and Farvolden*, 1979] in highly fractured systems [*Gleeson et al*., 2009], with seasonal frozen ground exerting an important control on the proportion of snowmelt recharging aquifers [*Granger et al*., 1984]. Indeed, field monitoring in Sweden [*Rodhe*, 1981], Idaho [*Flerchinger et al*., 1992], and the United States midwest [*Delin et al*., 2007; *Dripps*, 2012] have found that the spring snowmelt constitutes the bulk of annual groundwater recharge.

In spite of the aforementioned examples, a seasonal difference in the groundwater recharge ratio has not been found in all cases (e.g., Spain) [*Leterme et al*., 2012], advocating for a broader, global analysis to test the spatial variability of season differences in the efficiency of groundwater recharge. Most critically, knowledge and synthesis of intra-annual groundwater recharge fluxes are needed for accurately assessing and forecasting how land use change and the ongoing intensification of the global water cycle [*Durack et al*., 2012] will impact future groundwater recharge rates.

The seasonality of groundwater recharge calculated using hydrological models is yet to be tested or validated at a global scale. While there exists a pressing need for a hydrometric-based global groundwater recharge network, such an undertaking would be prohibitively expensive with today's measurement technology. Here we explore a new method for quantifying the seasonality of global groundwater recharge using readily available precipitation-isotopic and groundwater-isotopic data. We hypothesize that by comparing the isotopic composition of groundwater to that of precipitation we can quantify the seasonality of the groundwater recharge ratio at a given location.

Previous hydrological investigations have found that the isotopic composition of annual precipitation is similar to the isotopic composition of groundwater in the UK [*Darling and Bath*, 1988; *Darling et al*., 2003], Finland [*Kortelainen and Karhu*, 2004], Korea [*Lee et al*., 1999; *Lee and Kim*, 2007], the northeastern United States [*Yonge et al*., 1985; *Van Beynen and Febbroriello*, 2006], China [*Li et al*., 2000], France [*Genty et al*., 2014], Italy [*Madonia et al*., 2013], Israel [*Even et al*., 1986], Tasmania [*Goede et al*., 1982], and New Zealand [*Williams and Fowler*, 2002] suggesting that the proportion of recharge to precipitation is similar for all months of the year. However, not all studies have shown a match between the isotopic composition of groundwater and precipitation. Differences between amount-weighted precipitation and modern groundwater isotopic compositions were first shown more than 50 years ago by *Vogel et al*. [1963] in South Africa. Subsequent studies noted similar offsets, with groundwater discovered to be isotopically depleted in ^{18}O and ^{2}H compared to annual precipitation in the south-western United States (Arizona [*Simpson et al*., 1972; *Kalin*, 1994], Nevada [*Winograd et al*., 1998]), the north-eastern United States (Pennsylvania [*O'driscoll et al*., 2005], Vermont [*Abbott et al*., 2000]), central Canada (Alberta) [*Maulé et al*., 1994; *Grasby et al*., 2010], southern Canada (Ontario) [*Huddart et al*., 1999], French Guyana [*Négrel and Giraud*, 2010], St. Croix [*Gill*, 1994], Spain [*Julian et al*., 1992], Barbados, Puerto Rico, and Guam [*Jones et al*., 2000; *Jones and Banner*, 2003].

The difference between precipitation and groundwater isotopic compositions is interpreted to be the result of higher groundwater recharge ratios (i.e., recharge/precipitation) during winter months in arid [*Simpson et al*., 1972; *Kalin*, 1994; *Winograd et al*., 1998] and seasonal climates [*Vogel et al*., 1963; *Maulé et al*., 1994; *Abbott et al*., 2000; *O'driscoll et al*., 2005], or the result of higher groundwater recharge ratios during the wet season in tropical and subtropical settings [e.g., *Jones et al*., 2000; *Jones and Banner*, 2003; *Négrel and Giraud*, 2010]. Such isotope patterns, if examined globally, could be a way to overcome the impossibility of mounting a global hydrometric network and provide data to confirm or deny intuitive hypotheses about the seasonality of groundwater recharge ratios—information critically needed for future global water security scenarios. The results of the individual groundwater-precipitation isotopic investigations have not yet been synthesized at a global scale, and in most cases the seasonality in groundwater recharge ratios has only been expressed qualitatively.

The objective of this study is to quantify seasonal differences in the groundwater recharge ratio by comparing the isotopic composition of groundwater to that of precipitation. Specifically, we quantify the seasonality of groundwater recharge ratios at 54 globally distributed locations that lie within a variety of biomes to test the relative importance of individual seasons for groundwater recharge. We then explore the regional controls on groundwater recharge ratios by examining specific sites in our 54-site synthesis and comparing our results with groundwater recharge estimates from published global hydrological model (PCR-GLOBWB) by *Wada et al*. [2010]. Finally, we outline the implications for this work for predicting future changes to groundwater recharge as climate change impacts the intensity and seasonality of precipitation differently [e.g., *Hayhoe et al*., 2004; *Vera et al*., 2006], for interpreting isotopic records of past climates, and for understanding seasonal couplings between ecosystem productivity and groundwater recharge and how each may change under future land use and climate scenarios.

2. Theory and Methods

We draw upon isotopic data for precipitation samples from regional and global monitoring networks [*Araguás-Araguás et al*., 2000; *Welker*, 2000; *Birks and Edwards*, 2009; *Welker*, 2012] and compare the precipitation isotopic data to nearby groundwater data from individually compiled works. Precipitation data were obtained from the International Atomic Energy Agency [e.g., *Araguás-Araguás et al*., 2000] and the United

Table 1. Locations of Paired Precipitation and Groundwater Isotopic Data

Country	Station	Data	Lon.	Lat.	Aquifer	n[a]	Reference
GF	Cayenne	IAEA	−52.4	4.8	Guyana shield	10	*Négrel and Giraud* [2010]
GU	Taguac	IAEA	144.8	13.6	Guam caves	3	*Jones and Banner* [2003]
BB	Seawell	IAEA	−59.5	13.1	Barbados aqfr.	29	*Jones et al.* [2000]
ID	Jakarta	IAEA	106.8	−6.2	Jakarta aqfr.	36	*Kagabu et al.* [2011]
IN	New Delhi	IAEA	77.2	28.6	Gangetic plain	24	*Das et al.* [1988] and *Lorenzen et al.* [2012]
TZ	Dar es Salaam	IAEA	39.2	−6.9	Coastal aqfr.	13	*Bakari et al.* [2012]
ET	Addis Ababa	IAEA	38.7	9.0	Akaki volcanics	24	*Demlie et al.* [2007]. *Kebede et al.* [2008]. *Rango et al.* [2010] and *Bretzler et al.* [2011]
US	Santa Maria	IAEA	−120.5	34.9	CA coast	28	www.waterqualitydata.us
IL	Beit Dagan	IAEA	34.8	32.0	Israel coast aqfr.	10	*Yechieli et al.* [2009]
IT	Pisa	IAEA	10.4	43.7	Pisa plain	4	*Grassi and Cortecci* [2005]
US	Trout Lake	USNIP	−89.7	46.1	Surficial aqfr.	210	www.waterqualitydata.us
US	Yellowstone	USNIP	−110.4	44.9	Alluvial aqfr.	12	www.waterqualitydata.us
US	Smith's Ferry	USNIP	−116.1	44.3	Idaho Batholith	43	*Schlegel et al.* [2009]
US	Lake Geneva	USNIP	−88.5	42.6	Surficial aqfr.	7	www.waterqualitydata.us
US	East MA	USNIP	−71.2	42.4	Surficial aqfr.	100	www.waterqualitydata.us
US	Niwot Saddle	USNIP	−105.6	40.1	Surficial aqfr.	9	www.waterqualitydata.us
US	Wye	USNIP	−76.2	38.9	Aquia aqfr.	3	*Aeschbach-Hertig et al.* [2002]
US	Purdue Agr.	USNIP	−87.5	38.7	Surficial aqfr.	3	www.waterqualitydata.us
US	Clinton Stn.	USNIP	−78.3	35.0	Atlantic plain	3	www.waterqualitydata.us
US	Caddo Valley	USNIP	−93.1	34.2	MI River valley	3	www.waterqualitydata.us
US	Coffeeville	USNIP	−89.8	34.0	MI Embayment	5	www.waterqualitydata.us
CA	Saturna	CNIP	−123.2	48.8	Surficial aqfr.	31	*Allen* [2004]
CA	Ottawa	CNIP	−75.7	45.3	Surficial aqfr.	100	*Praamsma et al.* [2009]
GB	Wallingford	IAEA	−1.1	51.6	London Chalk	61	*Elliot et al.* [1999] and *Darling et al.* [1997]
PT	P. Douradas	IAEA	−7.6	40.4	Serra da Estrela	56	*Carreira et al.* [2011]
PL	Krakow	IAEA	19.9	50.1	Malm Limestones	27	*Zuber et al.* [2004] and *Samborska et al.* [2013]
DE	Cuxhave	IAEA	8.7	53.9	N. German Bsn.	3	*Kloppman et al.* [1998]
FR	Orleans	IAEA	1.9	47.9	Paris Bsn.	6	*Kloppman et al.* [1998]
AU	Melbourne	IAEA	145.0	−37.8	Yarra Bsn.	32	*Tweed et al.* [2005]
US	Newcastle	IAEA	−104.2	43.9	Surficial aqfr.	28	www.waterqualitydata.us
US	Little Bighorn	USNIP	−107.4	45.6	Surficial aqfr.	8	www.waterqualitydata.us
US	Lamberton	USNIP	−95.3	44.2	Mt. Simon aqfr.	46	*Berg and Person* [2011] www.waterqualitydata.us
US	N. Platte Agr.	USNIP	−100.8	41.1	N. High plains	19	*McMahon et al.* [2007]
US	Mon Mouth	USNIP	−90.7	40.9	Surficial aqfr.	5	www.waterqualitydata.us
US	Great Plains	USNIP	−97.5	35.0	Arbuckle aqfr.	4	www.waterqualitydata.us
CA	Edmonton	CNIP	−113.5	53.6	Surficial aqfr.	57	*Maulé et al.* [1994]
CA	Saskatoon	CNIP	−106.6	52.1	Dalmeny aqfrs.	3	*Fortin et al.* [1991]
CA	Wynyard	CNIP	−104.2	51.8	Surficial aqfr.	3	Unpublished data
CA	Esther	CNIP	−110.2	51.7	Surficial aqfr.	6	*Wallick* [1981]
CA	Calgary	CNIP	−114.0	51.0	Surficial aqfr.	32	*Lanza* [2009], *Cheung and Mayer* [2009], and *Rock and Mayer* [2009]
CA	Icelandic Park/Gimli	USNIP/CNIP	−97.8	48.8	Winnipeg fm.	27	*Ferguson et al.* [2007]
US	Craters of the Moon	USNIP	−113.6	43.5	Surficial aqfr.	3	www.waterqualitydata.us
US	Pinedale	USNIP	−109.8	42.9	Colorado Plat.	4	www.waterqualitydata.us
US	Sand Spring	USNIP	−107.7	40.5	Surficial aqfr.	20	www.waterqualitydata.us
US	Smith Valley	USNIP	−119.3	38.8	Basin and Range	161	www.waterqualitydata.us
US	Tuscon	[b]	−110.8	32.2	Tucson Basin	34	*Cunningham et al.* [1998]
MX	Chihuahua	IAEA	−106.1	28.6	Chihuahua plain	4	*Wassenaar et al.* [2009]
AU	Alice Springs	IAEA	133.9	−23.8	Amadeus Bsn.	8	*Wischusen et al.* [2004]
CN	Zhangye	IAEA	100.4	38.9	Hexi Corridor	33	*Qin et al.* [2011]
CN	Yinchuan	IAEA	106.2	38.5	Yinchuan plain	25	*Wang et al.* [2013]
CA	Yellowknife	CNIP	−114.3	62.3	Con mine	6	*Douglas et al.* [2000]
CA	Whitehorse	CNIP	−135.1	60.7	Surficial aqfr.	49	*Carey and Quinton* [2005]
CA	Chapais	CNIP	−75.0	49.8	Surficial aqfr.	3	*Boutin* [2009]

[a] *n* refers to the number of groundwater samples analyzed for $\delta^{18}O$ values at each location.
[b] Precipitation data from *Kalin* [1994].

States [*Welker*, 2000; *Vachon et al.*, 2010; *Welker*, 2012] and Canadian [*Birks and Edwards*, 2009] Network(s) for Isotopes in Precipitation. Groundwater isotopic data were compiled from 42 previously published data sets; the original references for each groundwater data set are presented in Table 1.

Herein, the ratios of $^{18}O/^{16}O$ and $^{2}H/^{1}H$ are referred to in delta notation and expressed in units of per mille (‰), where $\delta = (R_{sample}/R_{SMOW} - 1)\times 1000$ and R is the ratio of $^{18}O/^{16}O$ or $^{2}H/^{1}H$ in standard mean ocean water ("SMOW") or the measured water sample ("sample").

The majority of groundwater studies compiled here report groundwater samples without continuous long-term monitoring (i.e., "grab-samples"). However, multiyear monitoring of groundwater $\delta^{18}O$ and $\delta^{2}H$ values completed in Finland [*Kortelainen and Karhu*, 2004], Italy [*Iacumin et al.*, 2009], the UK [*Darling et al.*, 2003], New Zealand [*Williams and Fowler*, 2002], eastern Canada [*Savard et al.*, 2007], and France [*Genty et al.*, 2014] has each found little change in groundwater $\delta^{18}O$ and $\delta^{2}H$ values on interannual and interdecadal time scales. The nearly constant groundwater isotopic compositions over decadal time scales are due to multiyear groundwater residence times as well as hydrodynamic dispersion within aquifers, and support our treatment of groundwater grab samples as integrated signatures of groundwater recharge.

In this section, we outline a three-tier approach to determine the seasonality of groundwater recharge ratios using stable O and H isotopic data for groundwater and precipitation. First, precipitation isotopic data are analyzed to determine the seasonal (two 6 month intervals) and annual amount-weighted isotopic compositions of precipitation (section 2.1). Second, groundwater data are selected to ensure potential impacts from both evaporation and paleowater mixing are removed from the data set (section 2.2). Third, precipitation and groundwater isotopic compositions are compared and applied to quantify the seasonality of the groundwater recharge ratio at 54 study locations (section 2.3). Last, we compare the seasonality of the groundwater recharge ratio obtained from our stable-isotope-based method with the output of the global hydrological model PCR-GLOBWB (section 2.4) [*Wada et al.*, 2010].

2.1. The Isotopic Composition of Precipitation

For each precipitation station two parameters were required for analysis of seasonal groundwater recharge ratios: (i) the amount-weighted isotopic composition of annual precipitation and (ii) the amount-weighted isotopic composition of precipitation for season 1 (defined as winter months in the extratropics, and the wet season in the tropics) and season 2 (defined as summer months in the extratropics, and the dry season in the tropics). The amount-weighted isotopic composition of precipitation ($\delta_{P(annual)}$) was determined for each year with at least 11 months of monitoring data following equation (1):

$$\delta_{P(annual)} = \frac{\sum_{i=1}^{12} \delta_{P(i)} P_i}{\sum_{i=1}^{12} P_i} \quad (1)$$

where $\delta_{P(i)}$ represents the monthly isotopic composition of precipitation during month i and P_i represents the amount of precipitation that took place during month i.

The amount-weighted isotopic composition of season 1 ($\delta_{P(season\ 1)}$; defined as October to March in the northern hemisphere extratropics, and the wettest consecutive 6 month interval in the tropics) and season 2 ($\delta_{P(season\ 2)}$; defined as April to September in the extratropics, and the driest consecutive 6 month interval in the tropics) precipitation was calculated following equations (2) and (3):

$$\delta_{P(season\ 1)} = \frac{\delta_{P(10)}P_{10} + \delta_{P(11)}P_{11} + \delta_{P(12)}P_{12} + \delta_{P(1)}P_1 + \delta_{P(2)}P_2 + \delta_{P(3)}P_3}{P_{10}+P_{11}+P_{12}+P_1+P_2+P_3} \quad (2)$$

$$\delta_{P(season\ 2)} = \frac{\delta_{P(4)}P_4 + \delta_{P(5)}P_5 + \delta_{P(6)}P_6 + \delta_{P(7)}P_7 + \delta_{P(8)}P_8 + \delta_{P(9)}P_9}{P_4+P_5+P_6+P_7+P_8+P_9} \quad (3)$$

For locations in the southern hemisphere (e.g., Melbourne, Australia), the winter and summer months were inverted such that equation (2) was used to calculate $\delta_{P(season\ 1)}$ and equation (3) was used to calculate $\delta_{P(season\ 2)}$. For tropical settings, the wettest 6 month interval was used to calculate $\delta_{P(season\ 1)}$ and the driest 6 months were used to calculate $\delta_{P(season\ 2)}$.

2.2. The Isotopic Composition of Modern Groundwaters

A compilation of groundwater $\delta^{18}O$ and $\delta^{2}H$ values, groundwater well depths, and ^{3}H and ^{14}C activities were used in this study from existing published works (Table 1). Compiled $\delta^{18}O$ and $\delta^{2}H$ values were applied to examine the seasonality of recharge, whereas ^{3}H and ^{14}C activities were used to constrain the age of groundwater. Before comparing precipitation and groundwater data, considerations were made for

(i) possible effects of evaporation during groundwater recharge, and (ii) possible shifts in $\delta^{18}O$ and $\delta^{2}H$ values related to paleoclimates recorded in fossil groundwaters. First, partially evaporated groundwater samples were removed from our analysis using the deuterium excess parameter [*Dansgaard*, 1964] because partial evaporation leads to changes in isotopic compositions along $\delta^{2}H/\delta^{18}O$ slopes of <8 (see detailed approach in supporting information S1) [*Friedman*, 1953; *Gibson et al.*, 2008]. Groundwater samples with a deuterium excess of <0 were not considered in this analysis. Second, groundwater ages in excess of ~10,000 years were removed from this analysis on the basis of ^{3}H, ^{14}C, and well depths because fossil groundwaters have different $\delta^{18}O$ and $\delta^{2}H$ values from those observed in modern groundwaters (see detailed approach in supporting information S2) [*Plummer*, 1993; *Edmunds and Milne*, 2001; *Grasby and Chen*, 2005; *Karro et al.*, 2004; *Ferguson et al.*, 2007; *Edmunds*, 2009; *Jiráková et al.*, 2011; *McIntosh et al.*, 2012; *Jasechko et al.*, 2012]. We also exclude aquifers having recharge contributions from losing reaches of rivers because streamflow sourced from higher elevations may have a different climate than that of precipitation measurement stations found downstream (e.g., Albuquerque, New Mexico) [*Plummer et al.*, 2004].

2.3. Isotope-Based Groundwater Recharge Ratios

Differences in the isotopic compositions of precipitation and groundwater are interpreted to derive from seasonal differences in the ratio of groundwater recharge as a proportion of precipitation. Below we describe a set of equations that can be applied to quantify seasonal differences in the groundwater recharge ratio using the isotopic composition of precipitation (monthly integrated samples) and groundwaters (one-time grab sample) at the same location.

The isotopic composition for mean annual, winter, and summer precipitation (section 2.1) and recently recharged groundwaters without influence of evaporation (section 2.2) are applied to quantify seasonal changes in recharge ratio between winter and summer by combining a water budget (equation (4)) and an isotopic mass balance (equation (5)):

$$P_{annual} = P_{season\ 1} + P_{season\ 2} \tag{4}$$

$$P_{annual}\delta_{P(annual)} = P_{season\ 1}\delta_{P(season\ 1)} + P_{season\ 2}\delta_{P(season\ 2)} \tag{5}$$

where P_{annual}, $P_{season\ 1}$, and $P_{season\ 2}$ represent the precipitation fluxes for annual, season 1 (i.e., winter in the extratropics and the wet season in the tropics), and season 2 (summer in the extratropics and the dry season in the tropics) monthly intervals. Similarly, $\delta_{P(annual)}$, $\delta_{P(season\ 1)}$, and $\delta_{P(season\ 2)}$ represent the amount-weighted isotopic compositions for annual, season 1, or season 2 intervals. Combining equations (4) and (5) yields an isotope-based solution for the contribution of season 2 (i.e., summer or dry season) rainfall to total annual precipitation:

$$\frac{P_{season\ 2}}{P_{annual}} = \frac{\delta_{P(annual)} - \delta_{P(season\ 1)}}{\delta_{P(season\ 2)} - \delta_{P(season\ 1)}} \tag{6}$$

Similarly, groundwater recharge (R) can be assessed through water (equation (7)) and isotopic (equation (8)) mass balance equations:

$$R_{annual} = R_{season\ 1} + R_{season\ 2} \tag{7}$$

$$R_{annual}\delta_{groundwater} = R_{season\ 1}\delta_{P(season\ 1)} + R_{season\ 2}\delta_{P(season\ 2)} \tag{8}$$

where R_{annual}, $R_{season\ 1}$, and $R_{season\ 2}$ are the annual, season 1, and season 2 recharge fluxes. $\delta_{Groundwater}$ represents the isotopic composition of recently recharged groundwater that has not been substantially modified by isotope effects associated with evaporation (sections 2.1 and 2.2). Combining equations (7) and (8) yields the contribution of season 2 recharge to the total annual recharge flux (equation (9))

$$\frac{R_{season\ 2}}{R_{annual}} = \frac{\delta_{groundwater} - \delta_{P(season\ 1)}}{\delta_{P(season\ 2)} - \delta_{P(season\ 1)}} \tag{9}$$

Combining equations (6) and (9) yields an isotope-based estimate for the recharge ratio during the summer (extratropics) or dry season (tropics; $R_{season\ 2}/P_{season\ 2}$; equation (10))

$$\frac{R_{season\ 2}}{P_{season\ 2}} = \frac{\delta_{groundwater} - \delta_{P(season\ 1)}}{\delta_{P(annual)} - \delta_{P(season\ 1)}}\left(\frac{R_{annual}}{P_{annual}}\right) \tag{10}$$

A similar derivation (i.e., equations (4)–(10)) can be made to calculate the recharge ratio during season 1 ($R_{season\ 1}/P_{season\ 1}$; equation (11)):

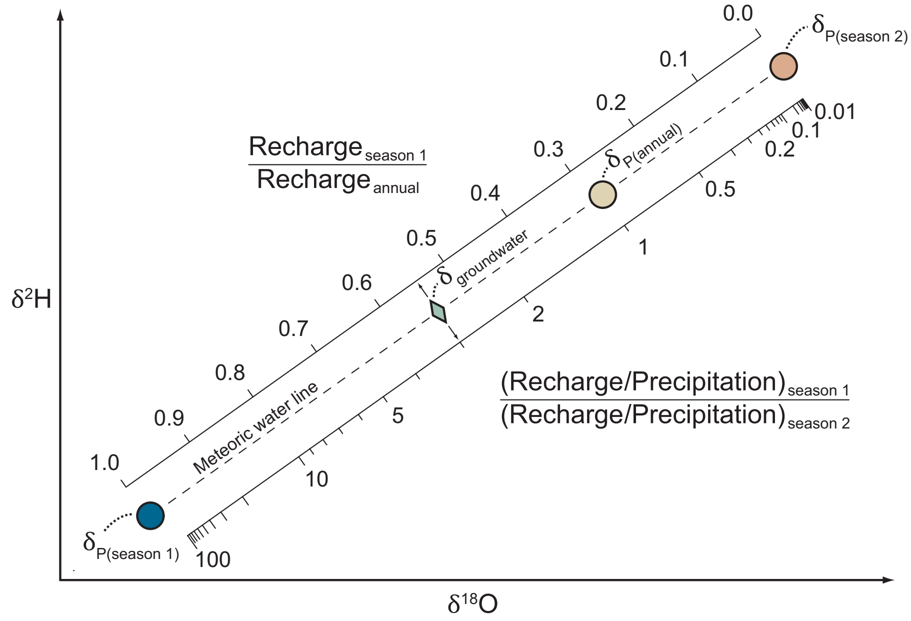

Figure 2. Schematic showing an isotope-based derivation of the seasonality of the groundwater recharge ratio (recharge as a proportion of precipitation: *R/P*). The upper axis marks the contribution of season 1 to the total annual recharge flux. The lower axis shows how a comparison of the isotopic composition of annual precipitation ($\delta_{P(annual)}$) and groundwater ($\delta_{Groundwater}$) can be used to compare the groundwater recharge ratios of season 1 (i.e., $(R/P)_{season\ 1}$) to season 2 (i.e., $(R/P)_{season\ 2}$). The example shown above (i) has 30% of the annual precipitation flux during season 2 ($\delta_{P(annual)}$ matched to upper axis), (ii) has 54% of the annual groundwater recharge during season 2 ($\delta_{Groundwater}$ matched to upper axis), and (ii) has a higher groundwater recharge ratio (i.e., *R/P*) during season 1 compared to season 2, with the $(R/P)_{season\ 1}/(R/P)_{season\ 2}$ value of 3 ($\delta_{Groundwater}$ matched to lower axis). The dashed line marks a hypothetical regression of meteoric waters for this specific location.

$$\frac{R_{season\ 1}}{P_{season\ 1}} = \frac{\delta_{groundwater} - \delta_{P(season\ 2)}}{\delta_{P(annual)} - \delta_{P(season\ 2)}} \left(\frac{R_{annual}}{P_{annual}} \right) \tag{11}$$

The contribution of a one season to the total annual recharge (i.e., $R_{season\ 1}/R_{annual}$, or, $R_{season\ 2}/R_{annual}$) is shown schematically in Figure 2 (upper axis). R_{annual} and P_{annual} can be obtained from global scale gridded estimates of recharge [*Wada et al*., 2010] to estimate recharge/precipitation ratios for individual seasons; however, an isotope-based comparison of season 1 and season 2 recharge ratios can be made without the knowledge of annual precipitation and recharge fluxes by combining equations (10) and (11):

$$\frac{(R/P)_{season\ 1}}{(R/P)_{season\ 2}} = \left(\frac{\delta_{groundwater} - \delta_{P(season\ 2)}}{\delta_{P(annual)} - \delta_{P(season\ 2)}} \right) \Big/ \left(\frac{\delta_{groundwater} - \delta_{P(season\ 1)}}{\delta_{P(annual)} - \delta_{P(season\ 1)}} \right) \tag{12}$$

yielding a fraction representing the seasonal difference in groundwater recharge ratios integrated over the recent past: $(R/P)_{season\ 1}/(R/P)_{season\ 2}$. This isotopic derivation of seasonal differences in groundwater recharge ratios is presented schematically in Figure 2 (lower axis).

Uncertainties were quantified by applying every combination of input data (i.e., every groundwater sample matched to every year that an amount-weighted isotopic composition of precipitation was available) and computing percentile ranges from the calculation results on a site-by-site basis. The calculation of seasonality in groundwater recharge ratios was only made for locations that had at least three groundwater δ^{18}O or δ^{2}H values and also had at least three annual amount-weighted δ^{18}O and δ^{2}H values for precipitation. Sixteen stations were not included in the analysis because either (i) no precipitation data were available for the summer or the winter season (examples: Damascus, Syria; N'Djamena, Chad; Hyderabad, India), or because (ii) the δ^{18}O and δ^{2}H values of winter and summer precipitation were not consistently higher or lower than the opposing season (examples: Entebbe, Uganda; Everglades National Park, Quincy and Kennedy Space Center in Florida, USA), negating the possibility of a two end-member mixing model. Comparisons of groundwater isotopic data and the amount-weighted isotopic composition of precipitation (for

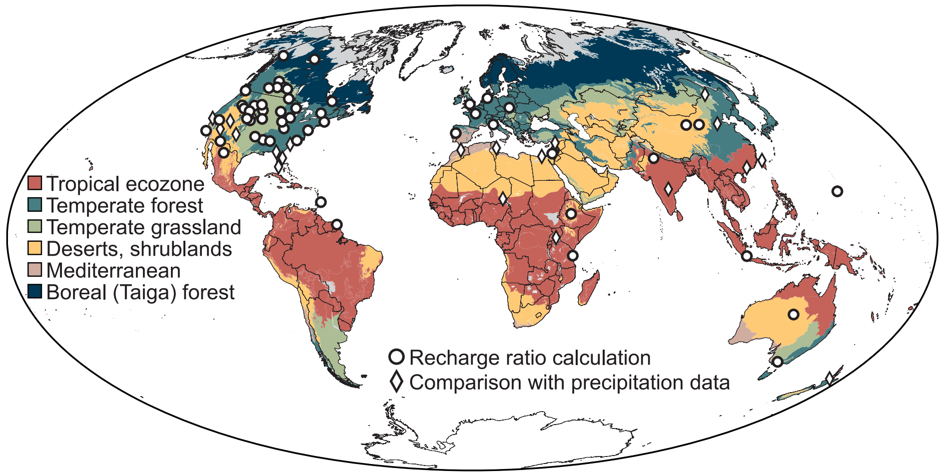

Figure 3. Locations where seasonal differences in recharge ratios (recharge/precipitation) are calculated on the basis of δ^{18}O and δ^2H values of precipitation and local groundwaters (white circles). White diamonds mark settings where a comparison of the isotopic compositions of groundwater and precipitation were made, but did not have sufficient data for a calculation of the groundwater recharge ratio.

each year with more than 10 months of data) were completed using a Welch t-test—that accounts for unequal variance between the precipitation and groundwater data (i.e., heteroscedastic)— to investigate the significance of differences between the two data pools: $\delta_{P(annual)}$ and $\delta_{Groundwater}$.

2.4. Model-Based Groundwater Recharge Ratios

Isotope-based groundwater recharge ratios were compared with outputs from the global hydrological model PCR-GLOBWB. Site-by-site isotope-based values of $(R/P)_{winter}$ and $(R/P)_{summer}$ were compared with modeled winter and summer average groundwater recharge ratios at the same location. The model itself integrates different hydrological processes occurring within the critical zone near to Earth's surface. In brief, the global hydrological model PCR-GLOBWB simulates for each grid cell (0.5° × 0.5° globally over the land) and for each time step (daily) the water storage in two vertically stacked soil layers and an underlying groundwater layer, as well as the water exchange between the layers (infiltration, percolation, and capillary rise) and between the top layer and the atmosphere (rainfall, evapotranspiration, and snowmelt). The model also calculates canopy interception and snow storage. Subgrid variability is taken into account by considering separately tall and short vegetation, open water (lakes, reservoirs, floodplains, and wetlands), different soil types, and the area fraction of saturated soil as well as the frequency distribution of groundwater depth. The groundwater layer represents the deeper part of the soil that is exempt from any direct influence of vegetation and constitutes a groundwater reservoir fed by active recharge. The groundwater store is explicitly parameterized based on lithology and topography, and represented as a linear reservoir model. For the detailed description, we refer to *Wada et al*. [2012a, 2012b].

3. Results

In this study, we quantify the seasonality of recharge at 54 globally distributed locations that lie within a variety of biomes to test the relative importance of individual seasons for groundwater recharge (Figure 3). Isotopic data for groundwater and the amount-weighted annual precipitation used to calculate groundwater recharge ratios are shown in Figure 4. Our isotope-based calculation of winter and summer groundwater recharge ratios (i.e., $(R/P)_{winter}/(R/P)_{summer}$) is shown in Figure 5 and Table 2.

Winter groundwater recharge ratios are higher than summer groundwater recharge ratios for the majority of deserts (7 of a total of 9), temperate grasslands (11 of a total of 13), and temperate forests (16 of a total of 18; median of δ^{18}O-based results calculated using every combination of annual-precipitation and groundwater isotopic data at each location; Figure 5). Winter groundwater recharge ratios are more than twice summer groundwater recharge ratios for half of all temperate grasslands and temperate forests (15 of the 31 locations) and for three quarters of deserts and xeric shrublands (7 of the 9 locations). Further, one

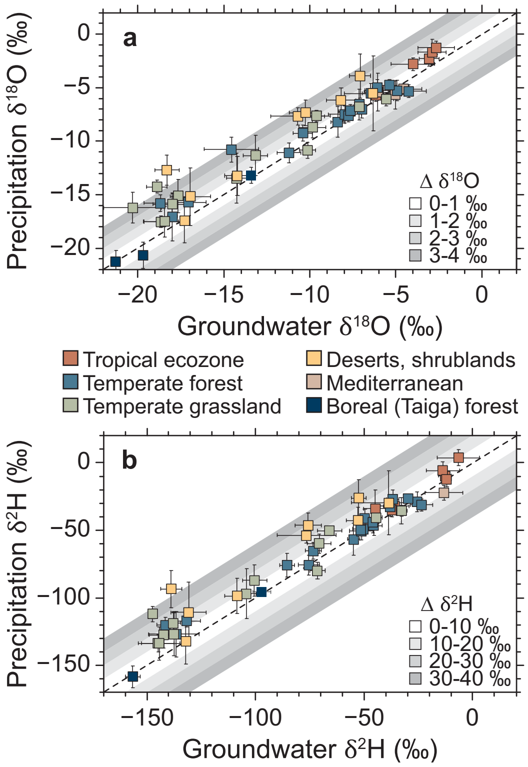

Figure 4. Isotopic compositions of precipitation and groundwater at 54 locations used in our calculation of groundwater recharge ratios. Precipitation δ^{18}O and δ^{2}H values are amount-weighted at a monthly time step. Error bars mark one standard deviation of interannual variability in the amount-weighted isotopic composition of precipitation and of all available groundwater data.

quarter of temperate or arid locations have a winter groundwater recharge ratio that is more than five times that of the summer.

Tropical groundwater recharge ratios were found to be much higher during the wet season relative to the dry season in all seven locations (i.e., $(R/P)_{wet} >> (R/P)_{dry}$; Figure 5). Only a few locations were available for Mediterranean climates ($n = 3$) and boreal forests ($n = 3$). Mediterranean climates examined here showed very little variability between summer and winter precipitation δ^{18}O and δ^{2}H values, resulting in highly uncertain isotope-based calculations of groundwater recharge ratios for these coastal locations (i.e., small change between $\delta_{P(summer)}$ and $\delta_{P(winter)}$; Figure 6). Boreal forests sites explored in the study ($n = 3$) show a similar groundwater recharge ratio during the summer and winter seasons.

4. Discussion

4.1. Comparison of Precipitation and Groundwater Isotopic Data

Recharge ratios were calculated for 54 aquifer-precipitation pairings that met all the criteria outlined in sections 2.1 and 2.2. Further, an additional 16 sites were available for a comparison of precipitation and groundwater δ^{18}O and δ^{2}H values, but were not suited for quantifying groundwater recharge ratios due to the lack of summer or winter precipitation end-members. Locations that were excluded from the recharge ratio calculation on the basis of indistinguishable summer and winter precipitation isotopic compositions are marked as diamonds in Figure 3. A comparison of δ^{18}O and δ^{2}H values for the amount-weighted isotopic composition of precipitation and groundwater is shown in Figure 7 for these 70 locations (average ± 1 SD uncertainty). Groundwater matched the amount-weighted precipitation from nearby monitoring stations within 1‰ for δ^{18}O and within 9‰ for δ^{2}H for half of the locations in this study, or within 2‰ for δ^{18}O and within 16‰ for δ^{2}H for the majority (80%) of study sites.

One third of the 70 aquifers have groundwater oxygen isotopic compositions that are significantly distinct ($p < 0.05$) from the isotopic composition of annual precipitation. Groundwater δ^{18}O values are lower than amount-weighted precipitation δ^{18}O values for 23 of the 24 locations having a statistically significant difference between annual precipitation and groundwater. For these locations, the difference between the precipitation and groundwater isotopic compositions ranged from $+1.8$‰ to -5.6‰ for δ^{18}O and from $+9$‰ to -45‰ for δ^{2}H. The closest match between the isotopic composition of groundwater and precipitation were found in regions with high overall δ^{18}O and δ^{2}H values. For example, all locations with average groundwater δ^{18}O values higher than -5‰ have amount-weighted precipitation values that match groundwater δ^{18}O values within 1.5‰. In contrast, regions with a lower groundwater δ^{18}O values have a broader range of differences between groundwater and precipitation. At locations where groundwater δ^{18}O values are < -10‰ ($n = 24$), the difference between groundwater and annual precipitation isotopic compositions (i.e., $\delta^{18}O_{Groundwater} - \delta^{18}O_{P(annual)}$) ranged between -5.6‰ and $+1.0$‰.

The larger difference between groundwater δ^{18}O and precipitation δ^{18}O found in regions with lower overall δ^{18}O values appears to be explained by spatial differences in the intra-annual fluctuations in precipitation isotopes. Regions that have higher δ^{18}O and δ^{2}H values also generally have more subdued seasonal fluctuations in the isotopic composition of precipitation (Figure 6). Conversely, regions with lower $\delta^{18}O_{P(annual)}$ and

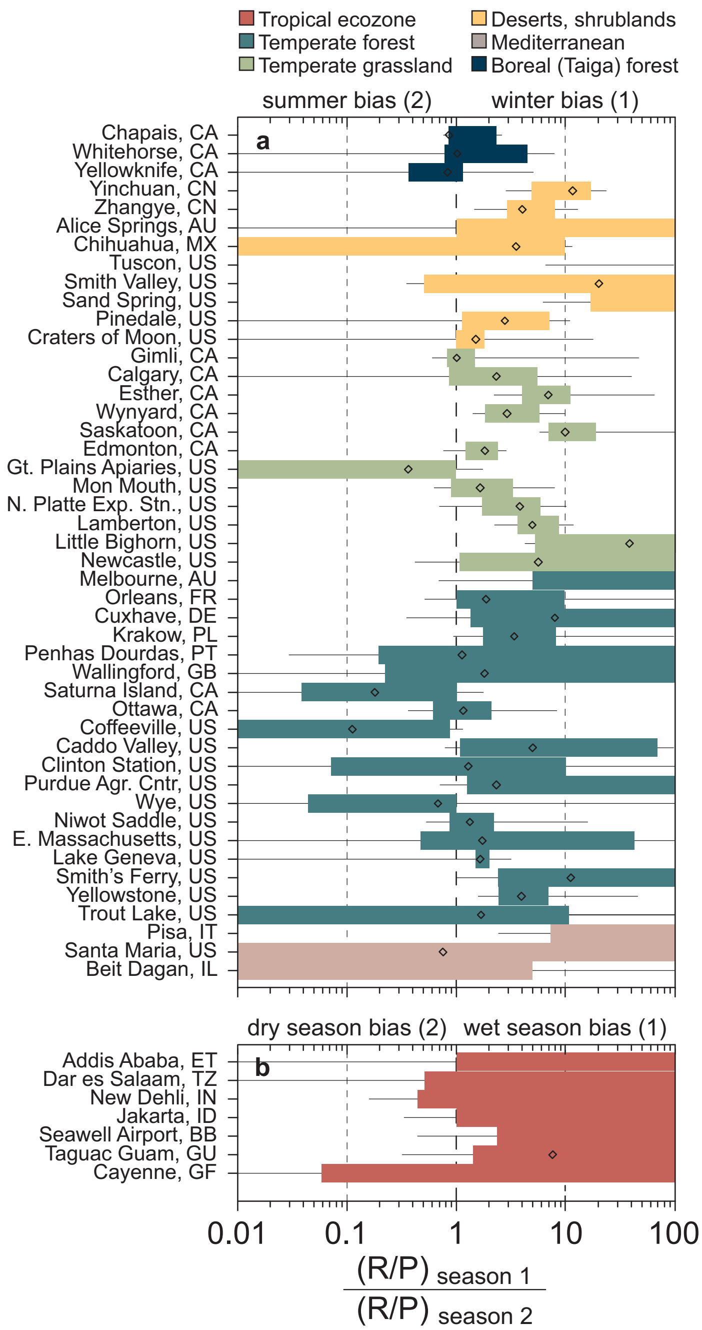

Figure 5. Seasonal differences in groundwater recharge ratios (recharge/precipitation: *R/P*) between the (a) summer and winter seasons (extratropics), or between the (b) wet and dry seasons (tropics) for 54 globally distributed locations. Winter is defined as October to March for northern hemisphere and April to September for southern hemisphere. Wet and dry seasons are defined as the wettest and driest consecutive 6 month interval for each tropical station. Colored bars mark the 25th–75th percentile range of results, whiskers mark the 10th–90th percentile range of calculation outputs, and black diamonds mark the median. The seasonality of groundwater recharge ratios shown here are from $^{18}O/^{16}O$-based results (results obtained from each tracer are similar in most cases because of the meteoric nature of groundwater).

$\delta^2H_{P(annual)}$ values tend to exhibit greater seasonal changes in the isotopic composition of precipitation. The difference between summer and winter precipitation isotopic compositions at 330 locations is shown in Figure 6 (data from *Araguás-Araguás et al.* [2000], *Welker* [2000], *Birks and Edwards* [2009], and *Liu et al.* [2013]). The difference between summer (April to September) and winter (October to March) $\delta^{18}O$ values is $<2‰$ for most stations that have an amount-weighted $\delta^{18}O_{P(annual)}$ value greater than $-3‰$ (i.e., 18 of the 19 stations). Conversely, the difference between summer and winter $\delta^{18}O$ values is $>5‰$ for most stations with an amount-weighted value of $<-15‰$ (i.e., 27 of the 31 stations). Geographically, stations located within the tropics have an average difference between winter and summer $\delta^{18}O$ values of 2.3‰ (SD of 1.6‰, $n = 46$), whereas locations in the extratropics have an average difference between winter and summer $\delta^{18}O$ values of 5.0‰ (SD of 4.0‰, $n = 176$).

Overall, it appears that groundwater values may be of use as a proxy for the long-term annual amount-weighted isotopic composition of precipitation in certain regions, reducing the need for long-term monitoring if only a long-term annual isotopic composition is sought. However, an offset should be applied when doing so as the majority of groundwaters have lower $\delta^{18}O$ and δ^2H values than annual precipitation. Further studies of the isotopic composition of modern groundwaters at the 330 locations shown in Figure 6 can help to better determine spatial differences in the difference between groundwater and precipitation and potentially develop predictive models for the isotopic composition of groundwater to complement existing global maps of the isotopic composition of precipitation [*Bowen and Wilkinson*, 2002; *Bowen and Revenaugh*, 2003].

Table 2. Seasonal Groundwater Recharge Ratio Results (Isotope-Based)

Country	Station	$\delta^{18}O$ P(annual)	δ^2H P(annual)	$\delta^{18}O_{P(summer)} - \delta^{18}O_{P(winter)}$	$\delta^2H_{P(summer)} - \delta^2H_{P(winter)}$	$\delta^{18}O$ groundwater	δ^2H groundwater	$(R/P)_{season\ 1}$ (%)[a]	$(R/P)_{season\ 2}$ (%)[c]
GF	Cayenne	−2.2	−10	1.4	4	−3.2	−13	0–39	0
GU	Taguac[b]	−5.3	−33	2.2	19	−6.2	−39	65–100	0–48
BB	Seawell[c]	−1.9	−6	1.8	13	−3.1	−16	17–35	0–6
ID	Jakarta	−5.6	−35	1.1	9	−6.1	−37	48–100	0–26
IN	New Delhi	−5.8	−38	5.0	41	−5.8	−45	11–23	0–21
TZ	Dar es Salaam	−2.6	−12	1.7	15	−4.1	−13	3.9–16	0
ET	Addis Ababa	−1.3	+3	0.9	9	−2.8	−6	29–96	0
US	Santa Maria	−5.0	−35	2.0	12	−4.9	−14	0–30	0–100
IL	Beit Dagan	−5.1	−22	1.7	6	−4.9	−33	0–15	0–34
IT	Pisa	−5.5	−33	0.7	n/a	−6.0	n/a	34–75	0–10
US	Trout Lake	−11.1	−77	6.1	49	−11.3	−86	0–100	9–67
US	Yellowstone	−16.2	−122	9.4	69	−18.9	−141	12–26	3.2–6
US	Smith's Ferry	−15.6	−118	4.9	36	−17.1	−132	11–16	0–5
US	Lake Geneva	−7.6	−53	4.5	32	−8.2	−54	33–39	21–24
US	East MA	−7.5	−51	2.2	25	−7.9	−51	17–56	0–30
US	Niwot Saddle	−17.6	−130	8.5	65	−18.0	−137	3.9–5	2.2–4.4
US	Wye	−7.3	−44	2.8	17	−7.1	−49	1.2–16	16–26
US	Purdue Agr.	−5.7	−33	3.4	24	−6.5	−39	22–40	0–18
US	Clinton Stn.	−5.0	−29	1.8	16	−4.8	−25	0–27	3.6–18
US	Caddo Valley	−4.9	−27	2.1	15	−5.5	−30	16–21	0.8–9
US	Coffeeville	−5.0	−32	1.5	12	−4.7	−26	0–24	21–72
CA	Saturna	−10.9	−79	2.2	14	−10.2	−72	6–57	64–100
CA	Ottawa	−11.0	−75	5.5	38	−11.3	−76	46–85	40–71
GB	Wallingford	−7.2	−49	1.5	10	−7.7	−51	15–54	0–25
PT	P. Douradas	−7.6	−45	0.9	6	−7.8	−46	12–42	0–39
PL	Krakow	−9.1	−65	3.8	29	−10.3	−72	22–38	4.4–13
DE	Cuxhave	−7.0	−49	1.4	9	−7.7	−52	22–51	0–17
FR	Orleans	−6.9	−46	1.8	13	−7.2	−46	0–16	0–6
AU	Melbourne	−5.0	−28	1.4	15	−6.1	−37	8–25	0–1.4
US	Newcastle	−11.2	−89	4.3	47	−13.1	−100	1.3–8	0–1.2
US	Little Bighorn	−15.1	−115	5.9	44	−17.6	−137	1.9–3.1	0–0.4
US	Lamberton	−7.6	−51	6.7	37	−9.6	−67	31–47	7–11
US	N. Platte Agr.	−9.0	−61	5.6	53	−10.1	−73	13–36	5–8
US	Mon Mouth	−6.7	−41	3.5	24	−7.1	−44	14–25	8–15
US	Great Plains	−5.8	−35	2.4	17	−5.6	−33	0–22	22–50
CA	Edmonton	−17.6	−131	10.6	84	−18.8	−146	68–100	43–56
CA	Saskatoon	−14.3	−111	9.0	76	−18.9	−152	up to 100	10–27
CA	Wynyard	−16.0	−124	7.8	62	−17.6	−140	78–100	33–52
CA	Esther	−15.7	−124	10.0	72	−20.3	−142	up to 100	17–37
CA	Calgary	−17.8	−138	8.6	49	−18.7	−146	48–100	36–63
CA	Gimli	−14.0	−102	11.3	72	−14.3	−105	4.1–6	4.4–5
US	Craters of Moon	−16.9	−128	3.3	52	−17.3	−132	0–0.1	0–0.1
US	Pinedale	−14.8	−110	9.9	38	−16.6	−128	6–14	2.1–6
US	Sand Spring	−12.8	−96	6.5	61	−18.2	−141	21–31	0–1.6
US	Smith Valley	−12.4	−94	3.8	24	−14.1	−108	33–100	0–55
US	Tuscon	−7.1	−53	2.5	8	−10.7	−77	13–25	0
MX	Chihuahua	−4.1	−26	6.1	42	−7.3	−54	0–18	0–2.4
AU	Alice Springs	−5.2	−22	1.6	20	−7.0	−46	0–15	0–0
CN	Zhangye	−6.7	−46	9.4	61	−8.0	−52	1.2–2.2	0.3–0.5
CN	Yinchuan	−7.4	−48	8.9	50	−10.2	−76	4.6–14	0–0.7
CA	Yellowknife	−20.7	−158	2.5	21	−19.7	−157	0–64	56–100
CA	Whitehorse	−21.3	−164	4.9	31	−21.3	n/a	48–100	25–66
CA	Chapais	−13.5	−97	5.2	45	−13.4	−97	54–100	44–64

[a]Annual recharge/precipitation fluxes from PCR-GLOBWB [*Wada et al.*, 2010, 2012a, 2012b, 2014]; the PCR-GLOBWB annual recharge/precipitation ratio has additional uncertainties not included in the range of values reported within these two columns.
[b]Taguac (Guam) recharge data from *Jocson et al.* [2002].
[c]Seawell (Barbados) recharge data from *Jones et al.* [2000].

4.2. Groundwater Recharge Ratios

Arid and temperate climates show higher winter recharge ratios than summer recharge ratios. This suggests that, from a groundwater recharge perspective, a given unit change in winter precipitation will be more important than the same unit change in summer precipitation.

The relatively high groundwater recharge ratios during the winter in arid and temperate climates may be due to intra-annual fluctuations in the evapotranspiration potential. Many of the arid and temperate

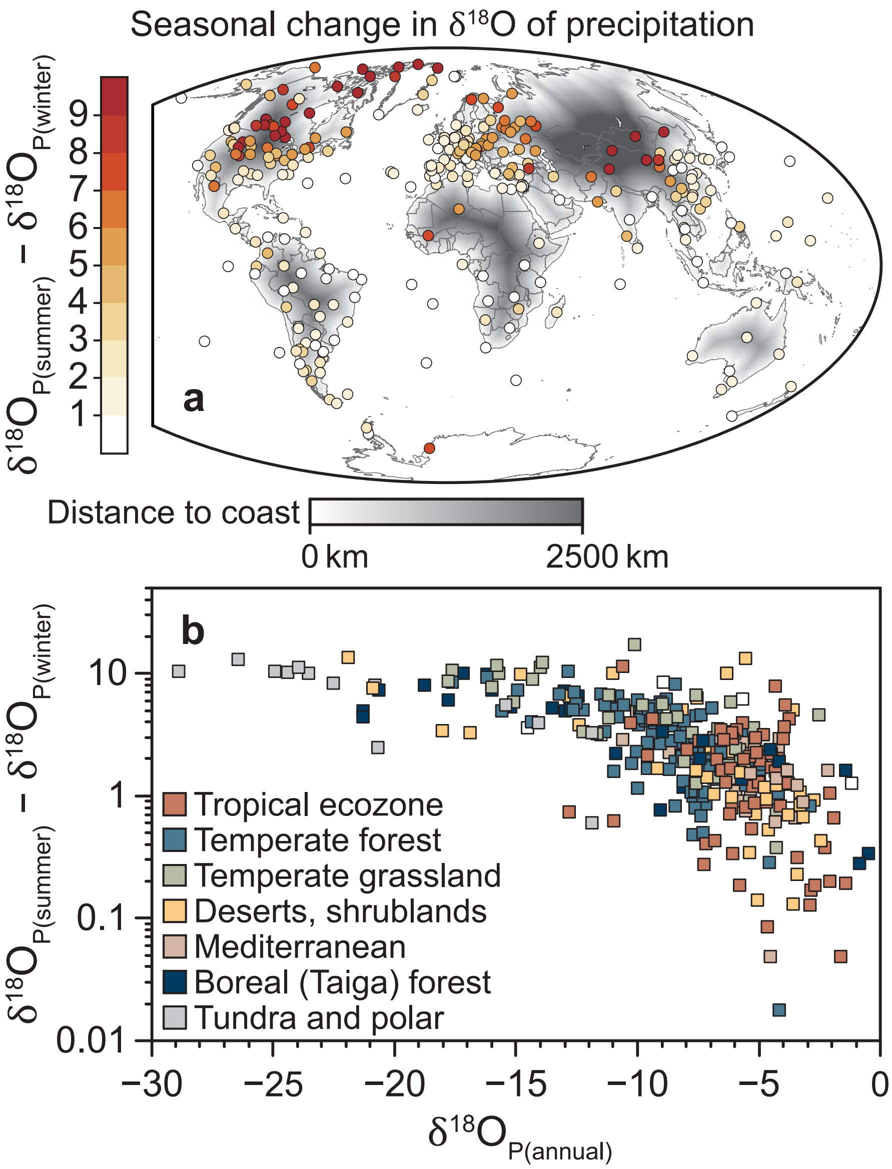

Figure 6. Absolute value of the difference between the precipitation-weighted δ^{18}O value of April to September and October to March ($\delta^{18}O_{P(summer)} - \delta^{18}O_{P(winter)}$) for 333 stations (absolute values shown, data sets obtained from *Welker* [2000], *Araguás-Araguás et al.* [2000], and *Birks and Edwards* [2009]) in (a) map form and (b) a cross-plot with the annual amount-weighted δ^{18}O of precipitation ($\delta^{18}O_{P(annual)}$). The largest seasonal differences in the δ^{18}O value of precipitation occur at high latitude and inland ("continental") settings characterized by low overall δ^{18}O values.

climates examined here are characterized by seasonal differences in surface temperature and plant growth. Lower summer recharge ratios are explained in part by the higher potential for evapotranspiration during the summer—which is broadly characterized by high temperatures, actively transpiring plants and greater potential for interception because of increased leaf area index. Higher winter recharge ratios are explained in part by the lower potential for evapotranspiration during the winter—which is broadly characterized by low atmospheric temperatures and dormant vegetation [*Welker et al.*, 1991; *Chimner and Welker*, 2005; *Blumenthal et al.*, 2008]. Figure 8 presents a global map of the seasonality in chlorophyll abundance, calculated using long-term monthly mean values of the normalized difference vegetation index (NDVI) to highlight the pronounced seasonal changes in plant growth. One quarter of continental areas—mostly located in the tropics—show less than a 10% difference between April to September and October to March NDVI values (stippled regions in Figure 8), suggesting the lack of a dominant growing season. Conversely, the greatest intra-annual changes in plant activity are found in cold regions (defined as having at least 1 month with a

10.1002/2014WR015809

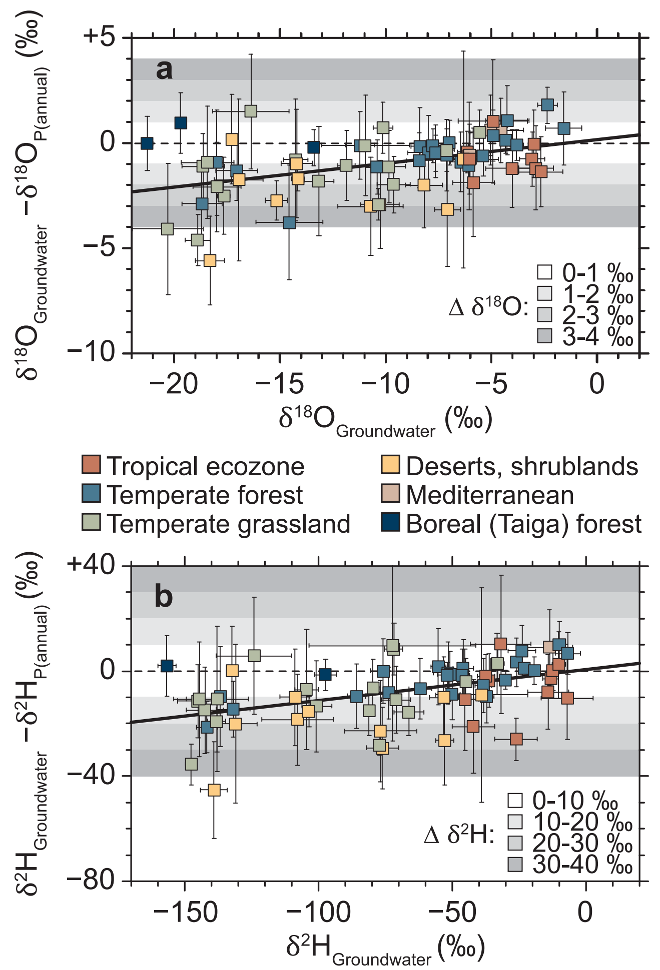

Figure 7. Differences in the stable oxygen and hydrogen isotopic compositions of amount-weighted precipitation ($\delta_{P(annual)}$) and local groundwaters ($\delta_{Groundwater}$). Error bars mark one standard deviation from the mean. Regressions of ($\delta_{P(annual)} - \delta_{Groundwater}$) and $\delta_{Groundwater}$ yield: ($\delta^{18}O_{P(annual)} - \delta^{18}O_{Groundwater}$) = (0.11 $\pm$ 0.02) $\times$ $\delta^{18}O_{\ Groundwater}$ + (0.17 $\pm$ 0.33) with $R^2 = 0.19$, and ($\delta^2H_{P(annual)} - \delta^2H_{Groundwater}$) = (0.12 $\pm$ 0.03) $\times$ $\delta^2H_{Groundwater}$ + (0.43 $\pm$ 2.32) with R^2 of 0.21 (standard errors shown as uncertainty). Both regressions (i.e., $\delta^{18}O$ and δ^2H) are significant at $p < 0.05$.

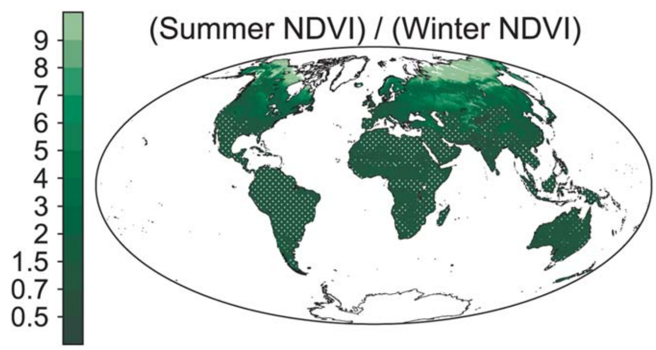

Figure 8. Seasonal changes in chlorophyll abundance (defined as the long-term mean summer NDVI divided by winter, where summer is an average of April to September for the northern hemisphere, or an average of October to March for the southern hemisphere; NDVI values of <0 were set to zero). Stippled areas mark regions where summer and winter NDVI values differ by <10% (i.e., (summer NDVI)/(winter NDVI) of between 0.91 and 1.1).

mean temperature <0°C) [*Bates and Bilello*, 1966], which cover one half of continental areas. Cold regions consistently have summertime NDVI values that are higher than winter NDVI values, whereas other regions have average NDVI values that are more consistent throughout the year (noncold-region $NDVI_{summer}/NDVI_{winter}$ with a global average value of 1; Figure 8), highlighting the more pronounced seasonality in plant growth in cold regions.

Some cold regions are characterized by seasonally frozen ground (i.e., a seasonal shallow confining unit) during the winter, which might be expected to inhibit winter recharge [*Hayashi et al.*, 2003; *Cable et al.*, 2013]. This potential seasonal blocking of recharge may have an effect, but overall it does not appear to be significant enough to override the seasonality of groundwater recharge ratios in temperate regions, as evident by the relatively high recharge/precipitation ratios during winter months. This effect may be offset by enhanced groundwater recharge during rapid melt of seasonal snowpack. Indeed, studies in the northern United States found that groundwater recharge is more than twice the monthly precipitation during spring freshet, implying that snowmelt constitutes a significant portion of annual recharge [*Dripps and Bradbury*, 2010; *Dripps*, 2012]. Additional work from Canada has shown that snowmelt provides an extremely rapid (i.e., hourly time scale) and efficient groundwater recharge mechanism [*Gleeson et al.*, 2009].

Fractionation of snowmelt potentially alters the sequential meltwater isotopic composition in cold regions [*Taylor et al.*, 2002; *Earman et al.*, 2006]. No attempt was made to quantify this potential effect because of limited quantitative knowledge of its importance. However, because the isotopic change to snowpack over time results in higher δ^{18}O and δ^{2}H values, including this effect into our calculation (i.e., $\delta_{P(season\ 1)}$ in equation (12)) would result in even higher winter recharge ratios. The potential for bias toward higher summer recharge ratios in our calculation (i.e., bias toward lower $(R/P)_{season\ 1}/(R/P)_{season\ 2}$ values) strengthens our finding that winter recharge ratios exceed summer recharge ratios.

There are four temperate locations in our analysis that have a summer recharge ratio that exceeds the winter recharge ratio: Coffeeville (Mississippi, southern United States), Great Plains Apiaries (Oklahoma, south-central United States), Saturna Island (British Columbia, western Canada), and Wye (Maryland, eastern United States). While the driver behind this observation is not clear, it is noteworthy that all of these locations do not have a large winter snowpack (i.e., $<$5 mm of snow-water equivalent in February, as obtained from long-term monthly mean data from passive microwave satellite products: www.globsnow.info) [*Pulliainen*, 2006; *Takala et al*., 2009]. For some locations that receive high amounts of winter rainfall (e.g., Saturna Island), wintertime storage may fill and inhibit winter recharge, generating runoff instead of recharge [*Sayama et al*., 2011]. This could in part help to explain the isotope-based observation of higher summer recharge ratios, although more detailed research in these locations is needed.

Tropical groundwater recharge ratios are higher during the wet season than the dry season in all cases examined, suggesting that larger and more intense rainfall leads to higher recharge/precipitation ratios. This finding is consistent with the previous isotope-based [*Jones et al*., 2000; *Jones and Banner*, 2003; *Muñoz-Villers and McDonnell*, 2012] and water-level monitoring (e.g., Namibia, Uganda, Ethiopia and Tanzania) [*Wanke et al*., 2008; *Owor et al*., 2009; *Walraevens et al*., 2009; *Taylor et al*., 2013] investigations that show that groundwater recharge is most efficient during high intensity rainfall events in the tropics. This finding implies that possible increases in the frequency of high-intensity rainfall events under a future—and currently intensifying [*Durack et al*., 2012]—water cycle might enhance groundwater resources in some tropical locations; however, this scenario may coincide with elevated risks to local communities (e.g., floods, landslides) [*Belle et al*., 2013].

Uncertainty ranges for isotope-based groundwater recharge ratios in tropical settings are larger than uncertainty ranges in regions with greater seasonality. The high uncertainty in $(R/P)_{season\ 1}/(R/P)_{season\ 2}$ values in the tropics is due to the relatively small difference between the isotopic composition of summer and winter precipitation (average of 1.9‰) compared to that of temperate (average of 4.9‰) and arid (average of 5.8‰) climates. Figure 6 shows the intra-annual variability in δ^{18}O values of precipitation. Inland and high-latitude locations are have greater seasonal changes in δ^{18}O and δ^{2}H values relative to coastal and tropical locations. The subdued intra-annual changes in δ^{18}O and δ^{2}H values in the tropics result in higher uncertainties in the calculation of seasonal changes in the groundwater recharge ratio, suggesting that the isotope-based approach to calculate groundwater recharge ratios will produce better constrained outputs in hydroclimates with pronounced seasonality. In spite of the high uncertainties in isotope-based tropical recharge/precipitation calculations (e.g., $(R/P_{wet\ season})/(R/P_{dry\ season})$ of $\sim$1 to $>$100 for the tropical locations examined here; Figure 5), there exist more than 60 tropical locations with long-term isotopic data for precipitation (International Atomic Energy Agency: www.iaea.org/water), presenting an opportunity to calculate groundwater recharge ratios should isotopic data for groundwater become available at these locations.

Boreal forests ($n = 3$) have a similar recharge ratio for summer and winter seasons, potentially related to the effects of perennially frozen ground and active layer controls upon recharge at the three sites that are situated within isolated, sporadic, and discontinuous permafrost zones [*Cable et al*., 2013]. The boreal settings show large seasonal differences between $\delta^{18}O_{P(summer)}$ and $\delta^{18}O_{P(winter)}$ (2.5–5.2‰; Table 2) compared to Mediterranean climates (0.7–2.0‰), suggesting that groundwater samples analyzed for stable O and H isotopes can be used to constrain seasonality in groundwater recharge ratios where long-term monitoring of the isotopic composition of precipitation have already been made (e.g., stations in the United States, Canadian and Russian Network(s) for isotopes in precipitation) [*Welker*, 2000; *Birks and Edwards*, 2009; *Kurita et al*., 2004].

4.3. Comparison With a Global Hydrological Model

Figure 9 shows a spatial comparison of the isotope-based groundwater recharge ratios with the outputs from a global hydrological model (PCR-GLOBWB) [*Wada et al*., 2010]. Median recharge/precipitation ratios obtained from the isotope-based approach fall within the range of PCR-GLOBWB outputs for more than half

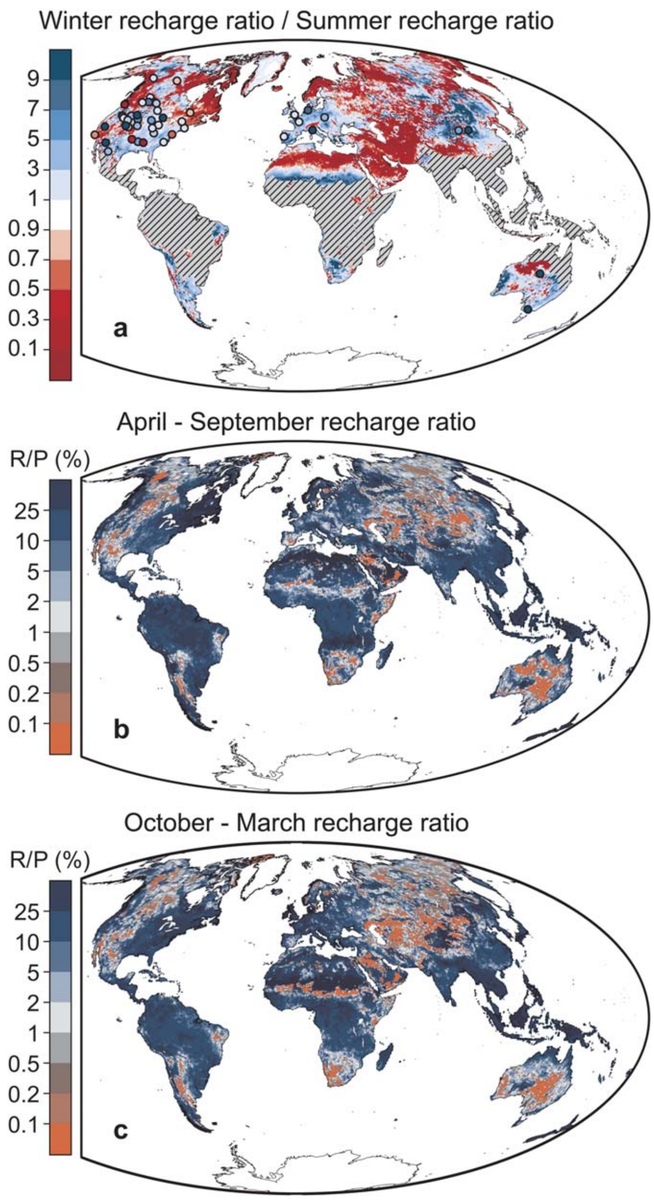

Figure 9. Seasonal differences in groundwater recharge ratios from the global hydrogeologic model *PCR-GLOBWB* [*Wada et al*., 2010]. (a) A comparison of winter and summer recharge ratios from PCR-GLOBWB for the extratropics (tropical regions grayed out with hatch marks). Median $(R/P)_{winter}/(R/P)_{summer}$ values from δ^{18}O-based results are shown in circles for comparison with model output. Figures 99b and 99c show 6 month average recharge ratios for (b) April to September and (c) October to March (c).

of all extratropical regions for both summer and winter seasons (range of modeled recharge/precipitation ratios within 100 km of each study location; Figure 10). Similarly, the 10th–90th percentile range of isotope-based recharge ratios overlaps with the range of modeled PCR-GLOBWB recharge ratios for 85% of extratropical locations.

The extratropical locations where the model *R*/*P* does not overlap within the 10th–90th percentiles of isotope-based *R*/*P* are found in regions that have between 18 and 81 mm of snow water equivalent stored as snow pack by February (i.e., Trout Lake and Craters of the Moon in the United States, and Edmonton, Saskatoon, Wynyard, and Esther in Canada, long-term monthly mean snowpack data from www.globsnow.info) [*Pulliainen*, 2006; *Takala et al*., 2009]. This difference may be partly explained by an important distinction between the isotope-based and model-based outputs. The isotope-based calculation assesses the seasonal distribution of recharge relative to the timing of precipitation, not necessarily the timing of recharge. For example, the recharge of snow that falls in the winter (October to March) but does not melt and infiltrate until later in the spring season (e.g., April to June) is included as winter recharge in the isotope-based calculation, even though the actual infiltration may occur during the timeframe defined as the summer in this study (i.e., "summer recharge" in PCR-GLOBWB). Other sources that may contribute to the observed differences include the irrigation of croplands that are not incorporated into PCR-GLOBWB as either a source of groundwater recharge, or as a predisposing mechanism that enhances the proportion of rainfall that can infiltrate the subsurface [*Chiew and McMahon*, 1991]. PCR-GLOBWB does not include focused recharge via lakes, wetlands, and rivers that may account for discrepancies in arid and semiarid regions where surface water bodies can be important sources of groundwater recharge.

4.4. Implications

Understanding the seasonal difference in the groundwater recharge ratio is important for many reasons. Here we outline the implications of our finding of higher groundwater recharge ratios during the winter (extratropics) and wet season (tropics) for predicting future groundwater recharge rates (section 4.4.1),

10.1002/2014WR015809

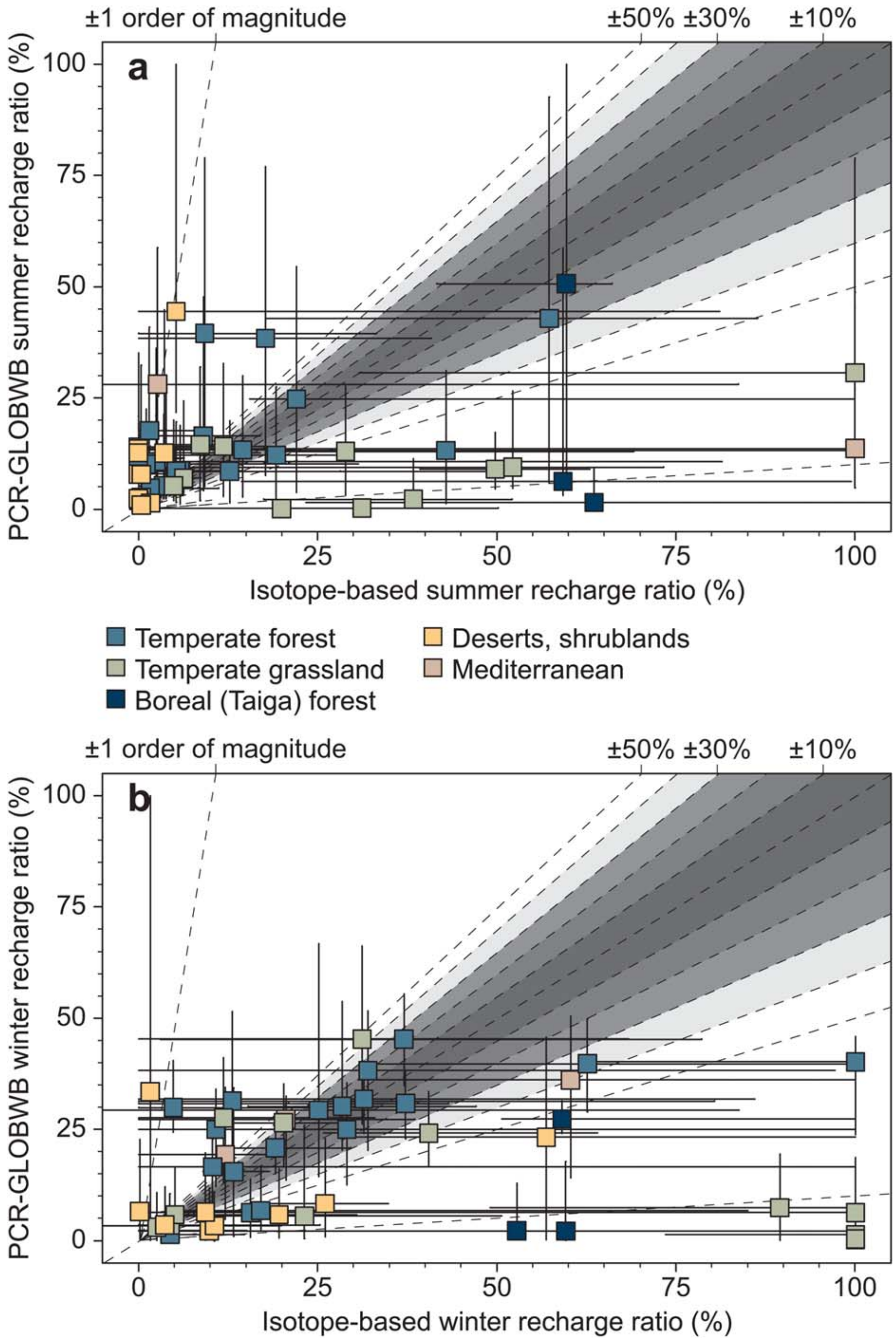

Figure 10. Comparison of recharge ratios calculated using isotope-based and hydrological modeling-based approaches for (a) summer (April to September) and (b) winter (October to March). Error bars (*x* axis) mark the 10th–90th percentile ranges for isotope-based calculations and squares mark the median result. Error bars on the *y* axis mark the range of model results within 100 km of each study location. Background shades delineate the percent difference between the isotope-based and modeling-based results (dashes mark one half order of magnitude and on order of magnitude differences). Colors for each square correspond to ecoregions as shown in the previous figures.

interpreting paleoclimate proxy records (section 4.4.2), and understanding plant-water interactions (section 4.4.3).

4.4.1. Implications: Groundwater Recharge in a Changing Climate

Existing projections of recharge have considerable uncertainties because of large differences between general circulation models, downscaling methods, and hydrological models [*Döll and Fielder*, 2008; *Wada et al.*, 2010; *Crosbie et al.*, 2011; *Portmann et al.*, 2013]. Several studies have assessed potential changes to groundwater recharge and found that different models range in the direction and magnitude of predicted changes on the order of approximately $\pm$20 to $\pm$50% [*Allen et al*., 2010; *Stoll et al*., 2011; *Dams et al*., 2012]. However, few models have assessed changes in the intra-annual distribution of groundwater recharge [*Dams et al*., 2012] suggesting that models may overlook important changes to individual seasons that will impact groundwater recharge. The isotopic approach presented here may be used to assess the most important seasonal hydrological processes governing groundwater recharge.

In temperate regions, we find that a higher percentage of winter precipitation is able to infiltrate and recharge aquifers relative to summer rainfall suggesting that a unit change to winter precipitation is more important than the same unit change to summer precipitation for groundwater recharge. Any changes in climate that impact either the amount of winter precipitation, or the summer precipitation deficit (i.e., precipitation minus evapotranspiration) could also impact the seasonality of the groundwater recharge, and consequently groundwater resources in extratropical areas. The bias toward winter recharge could also be altered if the hydrological processes that limit summer recharge change (e.g., summer evapotranspiration, summer storm intensities). The observed bias toward winter precipitation recharge in extratropical regions has been attributed to seasonal filtering of precipitation, with a greater proportion of winter precipitation reaching the water table relative to summer precipitation due to the high evapotranspiration rates that limit the amount of summer precipitation that recharges. The pronounced seasonality of groundwater recharge ratios discovered here is consistent with seasonal differences in runoff ratios, where the fraction of precipitation entering streams (i.e., the runoff ratio) is higher during winter than during the summer [*Dettinger and Diaz*, 2000].

For tropical settings, our results of higher groundwater recharge ratios during the rainy season supports integration of rainfall intensity and intra-annual distribution into forecasts of groundwater recharge in a warming climate. Site-specific modeling for Uganda has shown that including intra-annual variability and rainfall intensity into estimates of future change in recharge modifies the groundwater recharge forecasts from a 55% decrease to, instead, a 53% increase in recharge [*Mileham et al*., 2009]. Given the large number of precipitation monitoring stations (e.g., 330 locations in Figure 6) and the equations described here, measurement of groundwater isotopic compositions near to existing precipitation isotope stations can and should be completed to quantify the seasonality of groundwater recharge ratios across all continents. Paired investigations of differences between precipitation and groundwater isotopic compositions at the same location could also be incorporated into isotope-enabled general circulation models (e.g., ECHAM: *Hoffman et al*., 1998; CCSM: *Noone and Simmonds*, 2002; IsoGSM: *Yoshimura et al*., 2003; GISS: *Schmidt et al*., 2007; LMDZ4: *Risi et al*., 2010; iLOVECLIM: *Roche*, 2013] to trace the seasonality of groundwater recharge and enhance projections of annual groundwater recharge fluxes under changing seasonal precipitation patterns.

The groundwater recharge ratio is by no means static. A changing climate will not only impact the seasonal distribution of precipitation, but may also impact the seasonal distribution of the recharge-ratio and runoff-ratio [e.g., *Eckhart and Ulbrich*, 2003]. Recent pan-continent syntheses of rainfall, snowfall, and streamflow fluxes have shown that the runoff ratio is a function of not only the amount of precipitation, but also its phase (i.e., rain or snow) [*Berghuijs et al*., 2014]; the groundwater recharge ratio may be equally sensitive to the fraction of annual precipitation falling as snow or changes to freeze-thaw dynamics near to Earth's surface [*Jyrkama and Sykes*, 2007]. Isotopic monitoring of groundwater and precipitation may help to track these changes; however, prolonged residence times and subsurface water mixing are likely to hamper the tracking of year-to-year shifts in the groundwater recharge ratio using an isotope-based approach.

4.4.2. Implications: Paleoclimatology

Our finding that groundwater recharge fluxes do not match precipitation fluxes one-to-one (Figures 4 and 7) has three implications for the interpretation of isotope-based paleoclimate proxies.

First, changes to seasonality in precipitation may not be recorded on a one-to-one basis in paleoclimate records as recorded in fossil groundwaters, smectite, tree rings, speleothems, and vein calcite [e.g., *Winograd et al*., 1992; *Plummer*, 1993; *McCarroll and Loader*, 2004; *Asmerom et al*., 2010; *Stevenson et al*., 2010, *Winnick et al*., 2013]. Because groundwater recharge is a more efficient process during the winter relative to the summer, paleoclimate records based on groundwaters may be more representative of changes in winter (or, wet season) climate, relative to summer (or, dry season). This finding could help to explain some of the discrepancies observed in fossil groundwaters and lake sediment records from nearby locations. For example, Owens Lake, California, records δ^{18}O shifts of up to 10‰ over the past 500,000 years [*Smith and Bischoff*, 1997; *Menking et al.*, 1997] whereas the calcite archive from nearby Devils Hole, Nevada—which derives δ^{18}O shifts from groundwater—records much smaller δ^{18}O fluctuations of <3‰ over the past 500,000 years [*Winograd et al.*, 1992].

Second, dramatic shifts in climate and biomes from the last glacial period to the modern—such as deserts found in Europe and Alaska during the last glacial period, for example [*Williams*, 2003]—may have modified the recharge ratios in these settings and induced changes in groundwater-based δ^{18}O values. Of particular interest are the observed similarities between precipitation and groundwater isotopic compositions in boreal region found in this study. The boreal biome shifted into much lower latitudes at the last glacial maximum and may have modified the seasonality of groundwater recharge ratios at this time [*Williams*, 2003]. However, more work is needed in boreal regions with long-term precipitation δ^{18}O and δ^{2}H data to investigate this further.

Third, the seasonal differences between summer and winter precipitation shown in Figure 6 provide some information for the range of δ^{18}O shifts in paleoclimate records that can be attributed to changes in the seasonality of precipitation. Seasonality is commonly discussed as a potential source of changes in the isotopic composition meteoric waters amongst other factors such as differences in paleo-ocean δ^{18}O, atmospheric and sea surface temperatures, and air mass trajectories. For example, a hypothetical, complete shutdown of precipitation from a single 6 month interval can account for a shift no greater than ~9‰ in δ^{18}O (much less in most regions), if the seasonality of precipitation δ^{18}O were similar in the past to today. Some lacustrine paleoclimatic records, which are also subject to isotope effects due to evaporation, show more than 9‰ variation during the Pleistocene (e.g., Owens Lake, California) [*Smith and Bischoff*, 1997], and this analysis may help to put quantitative bounds on the magnitudes of δ^{18}O and δ^{2}H shifts that can be prescribed to seasonality when interpreting paleoclimate records.

4.4.3. Implications: Ecosystem Ecology

Finally, the groundwater recharge ratio patterns assessed here span a variety of biomes with different plant life forms, providing insight as to the mechanisms that may influence the temporal and spatial partitioning of water sources by vegetation with different life histories, rooting, and growth patterns [*Ehleringer and Cooper*, 1992; *Dodd et al.*, 1998; *Alstad et al.*, 1999; *Welker*, 2000; *Dawson et al.*, 2002; *Kulmatiski et al.*, 2010; *Leffler and Welker*, 2013]. In biomes such as deserts, temperate grasslands and temperate forests, seasonal hydrological processes facilitate the growth of a diversity of life forms (grasses and shrubs, trees, and understory plants) that utilize soil water and groundwater resources from different depths and are thus closely linked to water movements in the near surface. Coupled hydrosphere-biosphere models predict that the seasonality of precipitation is closely related to both annual evapotranspiration and ecosystem productivity, and is therefore linked to the fraction of precipitation available for groundwater recharge [*Feng et al.*, 2012]. Improved understanding of seasonal changes in vegetation characteristics and associated feedbacks to infiltration (e.g., interception, transpiration, rooting depth, and hydraulic redistribution) will help to better predict how large-scale ecosystem changes may impact groundwater recharge. For example, ongoing tree death due to mountain pine beetle infestation has recently been shown to reduce transpiration fluxes, resulting in a one third increase in groundwater fluxes that becomes particularly apparent in late summer [*Bearup et al.*, 2014]. Changing seasonality in groundwater recharge fluxes due to vegetation shifts has significant implications for aquatic species that depend upon groundwater refugia for habitat [e.g., *Power et al.*, 1999]. Further site-specific monitoring of groundwater and precipitation isotopic compositions can help to quantify vegetation water sources and to assess ecohydrological feedbacks under changing transpiration fluxes and plant water use efficiencies [*Keenan et al.*, 2013].

5. Conclusions

While the seasonality of groundwater recharge is highly intuitive, no synthetic data exist to quantify these patterns and evaluate model predictions. In this article we derived isotope-mass-balance equations that can be applied to quantify seasonal differences in the groundwater recharge ratio, which we define as the ratio of recharge as a proportion of incident precipitation. We applied this approach to a new synthesis of 54 globally distributed locations using previously reported precipitation and groundwater data sets. Our work has shown that the groundwater recharge ratio is higher during the winter than in the summer in arid and temperate climates, and highest during the rainy season in the tropics. The pronounced seasonality of groundwater recharge ratios implies that changes to winter (extratropics) and wet season (tropics) precipitation will produce a larger change to annual groundwater recharge fluxes than the same unit change to summer or dry season precipitation.

Acknowledgments
The authors are grateful for W. Dripps and K. Luojus for sharing hydrological modeling and snow water equivalent data. We are grateful for the time and insights contributed by M. Plummer and two anonymous reviewers that enhanced this publication. Original data sets analyzed within this study are available within the references listed in Table 1. S. Jasechko is grateful for the support of the American Geophysical Union's Horton Research Grant program, the Consortium of Universities for the Advancement of Hydrologic Science's Pathfinder Fellowship program, and a Caswell Silver Foundation graduate fellowship for support of this research. Support from NSF for the US Network for Isotopes in Precipitation (USNIP) in ESH 0080952 and MRI 0923571 awarded to J.M. Welker have been instrumental in the project success.

References

Abbott, M. D., A. Lini, and P. R. Bierman (2000), δ^{18}O, δD and ^{3}H measurements constrain groundwater recharge patterns in an upland fractured bedrock aquifer, Vermont, USA, *J. Hydrol.*, *228*, 101–112.

Aeschbach-Hertig, W., and T. Gleeson (2012), Regional strategies for the accelerating global problem of groundwater depletion, *Nat. Geosci.*, *5*, 853–861.

Aeschbach-Hertig, W., M. Stute, J. F. Clark, R. F. Reuter, and P. Schlosser (2002), A paleotemperature record derived from dissolved noble gases in groundwater of the Aquia Aquifer (Maryland, USA), *Geochim. Cosmochim. Acta*, *66*, 797–817.

Allen, D. M. (2004), Sources of ground water salinity on islands using ^{18}O, ^{2}H, and ^{34}S, *Ground Water*, *42*, 17–31.

Allen, D. M., A. J. Cannon, M. W. Toews, and J. Scibek (2010), Variability in simulated recharge using different GCMs, *Water Resour. Res.*, *46*, W00F03, doi:10.1029/2009WR008932.

Alstad, K. P., J. M. Welker, S. Williams, and M. J. Trilica (1999), Carbon and water relations of Salix monticola in response to winter browsing and changes in surface water hydrology: An isotopic study using δ^{13}C and δ^{18}O, *Oecologia*, *120*, 375–385.

Araguás-Araguás, L., K. Froehlich, and K. Rozanski (2000), Deuterium and oxygen-18 isotope composition of precipitation and atmospheric moisture, *Hydrol. Processes*, *14*, 1341–1355.

Asmerom, Y., V. J. Polyak, and S. J. Burns (2010), Variable winter moisture in the southwestern United States linked to rapid glacial climate shifts, *Nat. Geosci.*, *3*, 114–117.

Bakari, S. S., P. Aagaard, R. D. Vogt, F. Ruden, M. S. Brennwald, I. Johansen, and S. Gulliksen (2012), Groundwater residence time and paleorecharge conditions in the deep confined aquifers of the coastal watershed, South-East Tanzania, *J. Hydrol.*, *466*, 127–140.

Bates, R. E., and M. A. Bilello (1966), Defining the cold regions of the northern hemisphere, *Tech. Rep. 178*, CRREL, Hanover, N. H.

Bearup, L., R. M. Maxwell, D. W. Clow, and J. E. McCray (2014), Hydrological effects of forest transpiration loss in bark beetle-impacted watersheds, *Nat. Clim. Change*, *4*, 481–486.

Belle, P., B. Aunay, S. Bernardie, G. Grandjean, B. Ladouche, R. Mazué, and J.-L. Join (2013), The application of an innovative inverse model for understanding and predicting landslide movements (Salazie cirque landslides, Reunion Island), *Landslides*, *11*(3), 343–355.

Berg, J. A., and S. R. Pearson (2011), South-central Minnesota groundwater monitoring of the Mt. Simon aquifer: Minnesota, Version 3.2, report, 92 pp., Dep. of Natl. Resour., Ecol. and Water Resour. Div., St. Paul, Minn.

Berghuijs, W. R., R. A. Woods, and M. Hrachowitz (2014), A precipitation shift from snow towards rain leads to a decrease in streamflow, *Nat. Clim. Change*, *4*, 583–586.

Birks, S. J., and T. W. D. Edwards (2009), Atmospheric circulation controls on precipitation isotope-climate relations in western Canada, *Tellus, Ser. B*, *61*, 566–576.

Blumenthal, D., R. Chimner, J. M. Welker, and J. Morgan (2008), Increased snow facilitates plant invasion in mixedgrass prairie, *New Phytol.*, *179*, 440–448.

Boutin, P. (2009), Etude geochmique des eaux souterraines à la mine joe mann, Chibougamau, Québec, MSc thesis, 141 pp., Univ. du Qué, Chicoutimi, Canada.

Bowen, G. J., and J. Revenaugh (2003), Interpolating the isotopic composition of modern meteoric precipitation, *Water Resour. Res.*, *39*(10), 1299, doi:10.1029/2003WR002086.

Bowen, G. J., and B. Wilkinson (2002), Spatial distribution of δ^{18}O in meteoric precipitation, *Geology*, *30*, 315–318.

Bretzler, A., K. Osenbrück, R. Gloaguen, J. S. Ruprecht, S. Kebede, and S. Stadler (2011), Groundwater origin and flow dynamics in active rift systems—A multi-isotope approach in the Main Ethiopian Rift, *J. Hydrol.*, *402*, 274–289.

Cable, J., K. Olge, D. Bolton, L. Bentley, V. Romonvsky, H. Iwata, Y. Harazona, and J. M. Welker (2013), Permafrost thaw affects boreal deciduous plant transpiration through increased soil water, deeper thaw, and warmer soils, *Ecohydrology*, *7*, 982–997.

Carey, S. K., and W. L. Quinton (2005), Evaluating runoff generation during summer using hydrometric, stable isotope and hydrochemical methods in a discontinuous permafrost alpine catchment, *Hydrol. Processes*, *19*, 95–114.

Carreira, P. M., J. M. Marques, J. E. Marques, H. I. Chaminé, P. E. Fonseca, F. M. Santos, R. M. Moura, and J. M. Carvalho (2011), Defining the dynamics of groundwater in Serra da Estrela Mountain area, central Portugal: An isotopic and hydrogeochemical approach, *Hydrogeol. J.*, *19*, 117–131.

Castle, S. L., B. F. Thomas, J. T. Reager, M. Rodell, S. C. Swenson, and J. S. Famiglietti (2014), Groundwater depletion during drought threatens future water security of the Colorado River Basin, *Geophys. Res. Lett.*, *41*, 5904–5911, doi:10.1002/2014GL061055.

Cheung, K., and B. Mayer (2009), Chemical and isotopic characterization of shallow groundwater from selected monitoring wells in Alberta: Part I: 2006–2007, *Alberta Environ. Rep.*, 88 pp., Edmonton, Canada.

Chiew, F. H. S., and T. A. McMahon (1991), Groundwater recharge from rainfall and irrigation in the Campaspe River Basin, *Soil Res.*, *29*, 651–670.

Chimner, R. A., and J. M. Welker (2005), Ecosystem respiration responses to experimental manipulations of winter and summer precipitation in a Mixedgrass Prairie, WY, USA, *Biogeochemistry*, *73*, 257–270.

Clark, I. D., and P. Fritz (1997), *Environmental Isotopes in Hydrogeology*, A. F. Lewis, N. Y.

Crosbie, R. S., W. R. Dawes, S. P. Charles, F. S. Mpelasoka, S. Aryal, O. Barron, and G. K. Summerell (2011), Differences in future recharge estimates due to GCMs, downscaling methods and hydrological models, *Geophys. Res. Lett.*, *38*, L11406, doi:10.1029/2011GL047657.

Cunningham, E. E., A. Long, C. Eastoe, and R. L. Bassett (1998), Migration of recharge waters downgradient from the Santa Catalina Mountains into the Tucson basin aquifer, Arizona, USA, *Hydrogeol. J.*, *6*, 94–103.

Dams, J., E. Salvadore, T. Van Daele, V. Ntegeka, P. Willems, O. Batelaan, and H. J. Hendricks Franssen (2012), Spatio-temporal impact of climate change on the groundwater system, *Hydrol. Earth Syst. Sci.*, *16*, 1517–1531.

Dansgaard, W. (1964), Stable isotopes in precipitation, *Tellus*, *16*, 436–468.

Darling, W. G., and A. H. Bath (1988), A stable isotope study of recharge processes in the English Chalk, *J. Hydrol.*, *101*, 31–46.

Darling, W. G., W. M. Edmunds, and P. L. Smedley (1997), Isotopic evidence for palaeowaters in the British Isles, *Appl. Geochem.*, *12*, 813–829.

Darling, W. G., A. H. Bath, and J. C. Talbot (2003), The O and H stable isotope composition of freshwaters in the British Isles. 2. Surface waters and groundwater, *Hydrol. Earth Syst. Sci.*, *7*, 183–195.

Das, B. K., Y. P. Kakar, H. Moser, and W. Stichler (1988), Deuterium and oxygen-18 studies in groundwater of the Delhi area, India, *J. Hydrol.*, *98*, 133–146.

Dawson, T. E., S. Mambelli, A. H. Plamboeck, P. H. Templer, and K. P. Tu (2002), Stable isotopes in plant ecology, *Annu. Rev. Ecol. Syst.*, *33*, 507–559.

Delin, G. N., R. W. Healy, D. L. Lorenz, and J. R. Nimmo (2007), Comparison of local-to regional-scale estimates of ground-water recharge in Minnesota, USA, *J. Hydrol.*, *334*, 231–249.

Demlie, M., S. Wohnlich, B. Gizaw, and W. Stichler (2007), Groundwater recharge in the Akaki catchment, central Ethiopia: Evidence from environmental isotopes (δ^{18}O, δ^{2}H and ^{3}H) and chloride mass balance, *Hydrol. Processes*, *21*, 807–818.

Dettinger, M. D., and H. F. Diaz (2000), Global characteristics of stream flow seasonality and variability, *J. Hydrometeorol.*, *1*, 289–310.

Dodd, M. B., W. K. Lauenroth, and J. M. Welker (1998), Differential water resource use by herbaceous and woody plants in a shortgrass steppe community, *Oecologia*, *117*, 504–512.

Döll, P., and K. Fiedler (2008), Global-scale modeling of groundwater recharge, *Hydrol. Earth Syst. Sci. Discuss.*, *4*, 4069–4124.

Douglas, M., I. D. Clark, K. Raven, and D. Bottomley (2000), Groundwater mixing dynamics at a Canadian Shield mine, *J. Hydrol.*, *235*, 88–103.

Dripps, W. R. (2012), An integrated field assessment of groundwater recharge, *Open Hydrol. J.*, *6*, 15–22.

Dripps, W. R., and K. R. Bradbury (2010), The spatial and temporal variability of groundwater recharge in a forested basin in northern Wisconsin, *Hydrol. Processes*, *24*, 383–392, doi:10.1002/hyp.7497.

Dunne, T., and L. B. Leopold (1978), Water in environmental planning, New York, 818 pp.

Durack, P. J., S. E. Wijffels, and R. J. Matear (2012), Ocean salinities reveal strong global water cycle intensification during 1950 to 2000, *Science*, *336*, 455–458.

Earman, S., A. R. Campbell, F. M. Phillips, and B. D. Newman (2006), Isotopic exchange between snow and atmospheric water vapor: Estimation of the snowmelt component of groundwater recharge in the southwestern United States, *J. Geophys. Res.*, *111*, D09302, doi:10.1029/2005JD006470.

Eckhardt, K., and U. Ulbrich (2003), Potential impacts of climate change on groundwater recharge and streamflow in a central European low mountain range, *J. Hydrol.*, *284*, 244–252.

Edmunds, W. M. (2009), Palaeoclimate and groundwater evolution in Africa-implications for adaptation and management, *Hydrol. Sci. J.*, *54*, 781–792.

Edmunds, W. M., and C. J. Milne (Eds.) (2001), *Palaeowaters in Coastal Europe: Evolution of Groundwater Since the Late Pleistocene*, Geol. Soc. of London, Bath, U. K.

Ehleringer, J. R., and T. A. Cooper (1992), On the role of orientation in reducing photoinhibitory damage in photosynthetic-twig desert shrubs, *Plant Cell Environ.*, *15*, 301–306.

Elliot, T., J. N. Andrews, and W. M. Edmunds (1999), Hydrochemical trends, palaeorecharge and groundwater ages in the fissured Chalk aquifer of the London and Berkshire Basins, UK, *Appl. Geochem.*, *14*, 333–363.

Even, H., I. Carmi, M. Magaritz, and R. Gerson (1986), Timing the transport of water through the upper vadose zone in a karstic system above a cave in Israel, *Earth Surf. Processes Landforms*, *11*, 181–191.

Famiglietti, J. S., M. Lo, S. L. Ho, J. Bethune, K. J. Anderson, T. H. Syed, S. C. Swenson, C. R. de Linage, and M. Rodell (2011), Satellites measure recent rates of groundwater depletion in California's Central Valley, *Geophys. Res. Lett.*, *38*, L03403, doi:10.1029/2010GL046442.

Feng, W., M. Zhong, J. M. Lemoine, R. Biancale, H. T. Hsu, and J. Xia (2013), Evaluation of groundwater depletion in North China using the Gravity Recovery and Climate Experiment (GRACE) data and ground-based measurements, *Water Resour. Res.*, *49*, 2110–2118, doi:10.1002/wrcr.20192.

Feng, X., G. Vico, and A. Porporato (2012), On the effects of seasonality on soil water balance and plant growth, *Water Resour. Res.*, *48*, W05543, doi:10.1029/2011WR011263.

Ferguson, G. A., R. N. Betcher, and S. E. Grasby (2007), Hydrogeology of the Winnipeg formation in Manitoba, Canada, *Hydrogeol. J.*, *15*, 573–587.

Flerchinger, G. N., K. R. Cooley, and D. R. Ralston (1992), Groundwater response to snowmelt in a mountainous watershed, *J. Hydrol.*, *133*, 293–311.

Foley, J. A., et al. (2011), Solutions for a cultivated planet, *Nature*, *478*, 337–342.

Fortin, G., G. van der Kamp, and J. A. Cherry (1991), Hydrogeology and hydrochemistry of an aquifer-aquitard system within glacial deposits, Saskatchewan, Canada, *J. Hydrol.*, *126*, 265–292.

Friedman, I. (1953), Deuterium content of natural waters and other substances, *Geochim. Cosmochim. Acta*, *4*, 89–103.

Genty, D., et al. (2014), Rainfall and cave water isotopic relationships in two South-France sites, *Geochim. Cosmochim. Acta*, *131*, 323–343.

Gibson, J. J., S. J. Birks, and T. W. D. Edwards (2008), Global prediction of δA and δ^{2}H-δ^{18}O evaporation slopes for lakes and soil water accounting for seasonality, *Global Biogeochem. Cycles*, *22*, GB2031, doi:10.1029/2007GB002997.

Gill, I. (1994), Groundwater geochemistry of the Kingshill aquifer system, St. Croix, *Environ. Geosci.*, *1*, 40–49.

Gleeson, T., K. Novakowski, and T. K. Kyser (2009), Extremely rapid and localized recharge to a fractured rock aquifer, *J. Hydrol.*, *376*, 496–509.

Gleeson, T., Y. Wada, M. F. Bierkens, and L. P. van Beek (2012), Water balance of global aquifers revealed by groundwater footprint, *Nature*, *488*, 197–200.

Goede, A., D. C. Green, and R. S. Harmon (1982), Isotopic composition of precipitation, cave drips and actively forming speleothems at three Tasmanian cave sites, *Helictite*, *20*, 17–29.

Granger, R. J., D. M. Gray, and G. E. Dyck (1984), Snowmelt infiltration to frozen Prairie soils, *Can. J. Earth Sci.*, *21*, 669–677.

Grasby, S. E., and Z. Chen (2005), Subglacial recharge into the Western Canada Sedimentary Basin—Impact of Pleistocene glaciation on basin hydrodynamics, *Geol. Soc. Am. Bull.*, *117*, 500–514.

Grasby, S. E., J. Osborn, Z. Chen, and P. R. Wozniak (2010), Influence of till provenance on regional groundwater geochemistry, *Chem. Geol.*, *273*, 225–237.

Grassi, S., and G. Cortecci (2005), Hydrogeology and geochemistry of the multilayered confined aquifer of the Pisa plain (Tuscany-central Italy), *Appl. Geochem.*, *20*, 41–54.

Hayashi, M., G. van der Kamp, and R. Schmidt (2003), Focused infiltration of snowmelt water in partially frozen soil under small depressions, *J. Hydrol.*, *270*, 214–229.

Hayhoe, K., et al. (2004), Emissions pathways, climate change, and impacts on California, *Proc. Natl. Acad. Sci. U. S. A.*, *101*, 12,422–12,427.

Heppner, C. S., J. R. Nimmo, G. J. Folmar, W. J. Gburek, and D. W. Risser (2007), Multiple-methods investigation of recharge at a humid-region fractured rock site, Pennsylvania, USA, *Hydrogeol. J.*, *15*, 915–927.

Hoffmann, G., M. Werner, and M. Heimann (1998), Water isotope module of the ECHAM atmospheric general circulation model: A study on timescales from days to several years, *J. Geophys. Res.*, *103*, 16,871–16,896.

Huddart, P. A., F. J. Longstaffe, and A. S. Crowe (1999), δD and δ^{18}O evidence for inputs to groundwater at a wetland coastal boundary in the southern Great Lakes region of Canada, *J. Hydrol.*, *214*, 18–31.

Iacumin, P., G. Venturelli, and E. Selmo (2009), Isotopic features of rivers and groundwater of the Parma Province (Northern Italy) and their relationships with precipitation, *J. Geochem. Explor.*, *102*, 56–62.

Jasechko, S., J. J. Gibson, S. J. Birks, and Y. Yi (2012), Quantifying saline groundwater seepage to surface waters in the Athabasca oil sands region, *Appl. Geochem.*, *27*, 2068–2076.

Jasechko, S., Z. D. Sharp, J. J. Gibson, S. J. Birks, Y. Yi, and P. J. Fawcett (2013), Terrestrial water fluxes dominated by transpiration, *Nature*, *496*, 347–350.

Jiráková, H., F. Huneau, H. Celle-Jeanton, Z. Hrkal, and P. L. La Coustumer (2011), Insights into palaeorecharge conditions for European deep aquifers, *Hydrogeol. J.*, *19*, 1545–1562.

Jocson, J. M. U., J. W. Jenson, and D. N. Contractor (2002), Recharge and aquifer response: Northern Guam lens aquifer, Guam, Mariana Islands, *J. Hydrol.*, *260*, 231–254.

Jones, I. C., and J. L. Banner (2003), Estimating recharge thresholds in tropical karst island aquifers: Barbados, Puerto Rico and Guam, *J. Hydrol.*, *278*, 131–143.

Jones, I. C., J. L. Banner, and J. D. Humphrey (2000), Estimating recharge in a tropical karst aquifer, *Water Resour. Res.*, *36*, 1289–1299.

Joodaki, G., J. Wahr, and S. Swenson (2014), Estimating the human contribution to groundwater depletion in the Middle East, from GRACE data, land surface models, and well observations, *Water Resour. Res.*, *50*, 2679–2692, doi:10.1002/2013WR014633.

Jukić, D., and V. Denić-Jukić (2009), Groundwater balance estimation in karst by using a conceptual rainfall-runoff model, *J. Hydrol.*, *373*, 302–315.

Julian, J., L. Araguás-Araguás, K. Rozanski, J. Benavente, J. Cardenal, M. C. Hidalgo, S. Garcia-Lopez, J. C. Martinez-Garrido, F. Moral, and M. Olias (1992), Sources of precipitation over south-eastern Spain and groundwater recharge: An isotopic study, *Tellus, Ser. B*, *44*, 226–236.

Jyrkama, M. I., and J. F. Sykes (2007), The impact of climate change on spatially varying groundwater recharge in the grand river watershed (Ontario), *J. Hydrol.*, *338*, 237–250.

Kagabu, M., J. Shimada, R. Delinom, M. Tsujimura, and M. Taniguchi (2011), Groundwater flow system under a rapidly urbanizing coastal city as determined by hydrogeochemistry, *J. Asian Earth Sci.*, *40*, 226–239.

Kalin, R. M. (1994), The hydrogeochemical evolution of the groundwater of the Tucson Basin with application to 3-dimensional groundwater flow modelling, PhD thesis, 510 pp., Univ. of Ariz. Press, Tucson, Ariz.

Karro, E., A. Marandi, and R. Vaikmäe (2004), The origin of increased salinity in the Cambrian-Vendian aquifer system on the Kopli Peninsula, northern Estonia, *Hydrogeol. J.*, *12*, 424–435.

Kebede, S., Y. Travi, A. Asrat, T. Alemayehu, T. Ayenew, and Z. Tessema (2008), Groundwater origin and flow along selected transects in Ethiopian rift volcanic aquifers, *Hydrogeol. J.*, *16*, 55–73.

Keenan, T. F., D. Y. Hollinger, G. Bohrer, D. Dragoni, J. W. Munger, H. P. Schmid, and A. D. Richardson (2013), Increase in forest water-use efficiency as atmospheric carbon dioxide concentrations rise, *Nature*, *499*, 324–327.

Kim, J. H., and R. B. Jackson (2012), A global analysis of groundwater recharge for vegetation, climate, and soils, *Vadose Zone J.*, *11*, doi:10.2136/vzj2011.0021RA.

Kloppmann, W., L. Dever, and W. M. Edmunds (1998), Residence time of Chalk groundwaters in the Paris Basin and the North German Basin: A geochemical approach, *Appl. Geochem.*, *13*, 593–606.

Konikow, L. F. (2011), Contribution of global groundwater depletion since 1900 to sea-level rise, *Geophys. Res. Lett.*, *38*, L17401, doi:10.1029/2011GL048604.

Konikow, L. F., and E. Kendy (2005), Groundwater depletion: A global problem, *Hydrogeol. J.*, *13*, 317–320, doi:10.1007/s10040-004-0411-8.

Kortelainen, N. M., and J. A. Karhu (2004), Regional and seasonal trends in the oxygen and hydrogen isotope ratios of Finnish groundwaters: A key for mean annual precipitation, *J. Hydrol.*, *285*, 143–157.

Kulmatiski, A., K. H. Beard, R. J. Verweij, and E. C. February (2010), A depth-controlled tracer technique measures vertical, horizontal and temporal patterns of water use by trees and grasses in a subtropical savanna, *New Phytol.*, *188*, 199–209.

Kurita, N., N. Yoshida, G. Inoue, and E. A. Chayanova (2004), Modern isotope climatology of Russia: A first assessment, *J. Geophys. Res.*, *109*, D03102, doi:10.1029/2003JD003404.

Kurylyk, B. L., K. T. B. MacQuarrie, and C. I. Voss (2014), Climate change impacts on the temperature and magnitude of groundwater discharge from shallow, unconfined aquifers, *Water Resour. Res.*, *50*, 3253–3274, doi:10.1002/2013WR014588.

Lanza, S. (2009), Groundwater anammox at an industrial site in Calgary, MSc thesis, 96 pp., Univ. of Calgary.

Lee, K. S., and Y. Kim (2007), Determining the seasonality of groundwater recharge using water isotopes: A case study from the upper North Han River basin, Korea, *Environ. Geol.*, *52*, 853–859.

Lee, K. S., D. B. Wenner, and I. Lee (1999), Using H-and O-isotopic data for estimating the relative contributions of rainy and dry season precipitation to groundwater: Example from Cheju Island, Korea, *J. Hydrol.*, *222*, 65–74.

Leffler, J., and J. M. Welker (2013), Long-term increases in snow elevate leaf N and photosynthesis in Salix arctica: Response to a snow fence experiment in NW Greenland, *Environ. Res. Lett.*, *8*, 025023.

Leterme, B., D. Mallants, and D. Jacques (2012), Sensitivity of groundwater recharge using climatic analogues and HYDRUS-1D, *Hydrol. Earth Syst. Sci.*, *16*, 2485–2497.

Li, B., D. Yuan, J. Qin, Y. Lin, and M. Zhang (2000), Oxygen and carbon isotopic characteristics of rainwater, drip water and present speleothems in a cave in Guilin area, and their environmental meanings, *Sci. China, Ser. D*, *43*, 277–285.

Liu, Z., G. J. Bowen, K. Yoshimura, and J. M. Welker (2013), Pacific North American teleconnection controls on precipitation isotopes (δ^{18}O) across the contiguous USA and adjacent regions: A GCM-Based Analysis, *J. Clim.*, *27*, 1046–1061.

Lorenzen, G., C. Sprenger, P. Baudron, D. Gupta, and A. Pekdeger (2012), Origin and dynamics of groundwater salinity in the alluvial plains of western Delhi and adjacent territories of Haryana State, India, *Hydrol. Processes*, *26*, 2333–2345.

Madonia, P., R. D'Aleo, C. Di Maggio, R. Favara, and A. Hartwig (2013), The use of shallow dripwater as an isotopic marker of seepage in karst areas: A comparison between Western Sicily (Italy) and the Harz Mountains (Germany), *Appl. Geochem.*, *34*, 231–239.

Maulé, C. P., D. S. Chanasyk, and K. Muehlenbachs (1994), Isotopic determination of snow-water contribution to soil water and groundwater, *J. Hydrol.*, *155*, 73–91.

McCarroll, D., and N. J. Loader (2004), Stable isotopes in tree rings, *Quat. Sci. Rev.*, *23*, 771–801.

McIntosh, J. C., M. E. Schlegel, and M. Person (2012), Glacial impacts on hydrologic processes in sedimentary basins: Evidence from natural tracer studies, *Geofluids*, *12*, 7–12.

McMahon, P. B., J. K. Bohlke, and C. P. Carney (2007), Vertical gradients in water chemistry and age in the northern High Plains aquifer, Nebraska, 2003, *U.S. Geol. Surv. Sci. Invest. Rep. 2006–5294*, 66 pp., U.S. Dep. of the Interior, Reston, Va.

Menking, K. M., J. L. Bischoff, J. A. Fitzpatrick, J. W. Burdette, and R. O. Rye (1997), Climatic/hydrologic oscillations since 155,000 yr BP at Owens Lake, California, reflected in abundance and stable isotope composition of sediment carbonate, *Quat. Res.*, *48*, 58–68.

Mileham, L., R. G. Taylor, M. Todd, C. Tindimugaya, and J. Thompson (2009), The impact of climate change on groundwater recharge and runoff in a humid, equatorial catchment: Sensitivity of projections to rainfall intensity, *Hydrol. Sci. J.*, *54*, 727–738.

Muñoz-Villers, L. E., and J. J. McDonnell (2012), Runoff generation in a steep, tropical montane cloud forest catchment on permeable volcanic substrate, *Water Resour. Res.*, *48*, W09528, doi:10.1029/2011WR011316.

Négrel, P., and E. P. Giraud (2010), Geochemistry, isotopic composition (δ^{18}O, δ^{2}H, ^{87}Sr/^{86}Sr, ^{143}Nd/^{144}Nd) in the groundwater of French Guiana as indicators of their origin, interrelations, *C. R. Géosci.*, *342*, 786–795.

Noone, D., and I. Simmonds (2002), Associations between δ^{18}O of water and climate parameters in a simulation of atmospheric circulation for 1979–95, *J. Clim.*, *15*, 3150–3169.

O'driscoll, M. A., D. R. DeWalle, K. J. McGuire, and W. J. Gburek (2005), Seasonal ^{18}O variations and groundwater recharge for three landscape types in central Pennsylvania, USA, *J. Hydrol.*, *303*, 108–124.

Owor, M., R. G. Taylor, C. Tindimugaya, and D. Mwesigwa (2009), Rainfall intensity and groundwater recharge: Empirical evidence from the Upper Nile Basin, *Environ. Res. Lett.*, *4*, 035009.

Pangle, L., J. W. Gregg, and J. J. McDonnell (2014), Rainfall seasonality and an ecohydrological feedback offset the potential impact of climate warming on evapotranspiration and groundwater recharge, *Water Resour. Res.*, *50*, 1308–1321, doi:10.1002/2012WR013253.

Plummer, L. N. (1993), Stable isotope enrichment in paleowaters of the southeast Atlantic Coastal Plain, United States, *Science*, *262*, 2016–2020.

Plummer, L. N., L. M. Bexfield, S. K. Anderholm, W. E. Sanford, and E. Busenberg (2004), Hydrochemical tracers in the middle Rio Grande Basin, USA: 1. Conceptualization of groundwater flow, *Hydrogeol. J.*, *12*, 359–388.

Portmann, F. T., P. Döll, S. Eisner, and M. Flörke, M. (2013), Impact of climate change on renewable groundwater resources: Assessing the benefits of avoided greenhouse gas emissions using selected CMIP5 climate projections, *Environ. Res. Lett.*, *8*, 024023.

Power, G., R. S. Brown, and J. G. Imhof (1999), Groundwater and fish-insights from northern North America, *Hydrol. Processes*, *13*, 401–422.

Praamsma, T., K. Novakowski, K. Kyser, and K. Hall (2009), Using stable isotopes and hydraulic head data to investigate groundwater recharge and discharge in a fractured rock aquifer, *J. Hydrol.*, *366*, 35–45.

Pulliainen, J. (2006), Mapping of snow water equivalent and snow depth in boreal and sub-arctic zones by assimilating space-borne microwave radiometer data and ground-based observations, *Remote Sens. Environ.*, *101*, 257–269.

Qin, D., Y. Qian, L. Han, Z. Wang, C. Li, and Z. Zhao (2011). Assessing impact of irrigation water on groundwater recharge and quality in arid environment using CFCs, tritium and stable isotopes, in the Zhangye Basin, Northwest China, *J. Hydrol.*, *405*, 194–208.

Rango, T., R. Petrini, B. Stenni, G. Bianchini, F. Slejko, L. Beccaluva, and T. Ayenew (2010), The dynamics of central Main Ethiopian Rift waters: Evidence from δD, δ^{18}O and ^{87}Sr/^{86}Sr ratios, *Appl. Geochem.*, *25*, 1860–1871.

Risi, C., S. Bony, F. Vimeux, and J. Jouzel (2010), Water-stable isotopes in the LMDZ4 general circulation model: Model evaluation for present-day and past climates and applications to climatic interpretations of tropical isotopic records, *J. Geophys. Res.*, *115*, D12118, doi:10.1029/2009JD013255.

Roche, D. M. (2013), δ^{18}O water isotope in the iLOVECLIM model (version 1.0)-Part 1: Implementation and verification, *Geosci. Model Dev. Discuss.*, *6*, 1481–1491.

Rock, L., and B. Mayer (2009), Identifying the influence of geology, land use, and anthropogenic activities on riverine sulfate on a watershed scale by combining hydrometric, chemical and isotopic approaches, *Chem. Geol.*, *262*, 121–130.

Rodell, M., I. Velicogna, and J. S. Famiglietti (2009), Satellite-based estimates of groundwater depletion in India, *Nature*, *460*, 999–1002.

Rodhe, A. (1981), Spring flood meltwater or groundwater? *Nord. Hydrol.*, *12*, 21–30.

Samborska, K., A. Różkowski, and P. Małoszewski, P. (2013), Estimation of groundwater residence time using environmental radioisotopes (^{14}C, T) in carbonate aquifers, southern Poland, *Isot. Environ. Health Stud.*, *49*, 73–97.

Savard, M. M., D. Paradis, G. Somers, S. Liao, and E. van Bochove (2007), Winter nitrification contributes to excess NO^{3-} in groundwater of an agricultural region: A dual-isotope study, *Water Resour. Res.*, *43*, W06422, doi:10.1029/2006WR005469.

Sayama, T., J. J. McDonnell, A. Dhakal, and K. Sullivan (2011), How much water can a watershed store? *Hydrol. Processes*, *25*, 3899–3908.

Siebert, S., J. Burke, J. M. Faures, K. Frenken, J. Hoogeveen, P. Döll, and F. T. Portmann (2010), Groundwater use for irrigation—A global inventory, *Hydrol. Earth Syst. Sci.*, *14*, 1863–1880.

Scanlon, B. R., K. E. Keese, A. L. Flint, L. E. Flint, C. B. Gaye, W. M. Edmunds, and I. Simmers (2006), Global synthesis of groundwater recharge in semiarid and arid regions, *Hydrol. Processes*, *20*, 3335–3370.

Scanlon, B. R., C. C. Faunt, L. Longuevergne, R. C. Reedy, W. M. Alley, V. L. McGuire, and P. B. McMahon (2012), Groundwater depletion and sustainability of irrigation in the US High Plains and Central Valley, *Proc. Natl. Acad. Sci. U. S. A.*, *109*, 9320–9325.

Schlegel, M. E., A. L. Mayo, S. Nelson, D. Tingey, R. Henderson, and D. Eggett (2009), Paleo-climate of the Boise area, Idaho from the last glacial maximum to the present based on groundwater δ^{2}H and δ^{18}O compositions, *Quat. Res.*, *71*, 172–180.

Schmidt, G. A., A. N. LeGrande, and G. Hoffmann (2007), Water isotope expressions of intrinsic and forced variability in a coupled ocean-atmosphere model, *J. Geophys. Res.*, *112*, D10103, doi:10.1029/2006JD007781.

Sklash, M. G., and R. N. Farvolden (1979), The role of groundwater in storm runoff. In: Back, W. and D. A. Stephenson (eds.), Contemporary Hydrogeology—The George Burke Maxey Memorial Volume, *Dev. Water Sci.*, *43*, 45–65.

Simpson, E. S., D. B. Thorud, and I. Friedman (1972), Distinguishing seasonal recharge to groundwater by deuterium analysis in southern Arizona, in *Proc. Reeding Symposium*, *International Association of Scientific Hydrology*, pp. 623–633, UNESCO-WMO, Gentbrugge, Belgium.

Smith, G. I., and J. L. Bischoff (Eds.) (1997), An 800,000-year Paleoclimatic Record from Core OL-92, Owens Lake, Southeast California, *Geol. Soc. of Am. Spec. Pap. 317*, 37–47.

Stevenson, B. A., E. Kelly, E. McDonald, A. Busacca, and J. M. Welker (2010), Oxygen isotope ratios in Holocene carbonates across a climatic gradient, eastern Washington State, USA: Evidence for seasonal effects on pedogenic mineral isotopic composition, *Holocene*, *20*, 575–583.

Steward, D. R., P. J. Bruss, X. Yang, S. A. Staggenborg, S. M. Welch, and M. D. Apley (2013), Tapping unsustainable groundwater stores for agricultural production in the High Plains Aquifer of Kansas, projections to 2110, *Proc. Natl. Acad. Sci. U. S. A.*, *110*, E3477–E3486.

Stoll, S., H. J. Franssen, M. Butts, and W. Kinzelbach (2011), Analysis of the impact of climate change on groundwater related hydrological fluxes: A multi-model approach including different downscaling methods, *Hydrol. Earth Syst. Sci.*, *15*, 21–38.

Takala, M., J. Pulliainen, S. J. Metsamaki, and J. T. Koskinen (2009), Detection of snowmelt using spaceborne microwave radiometer data in Eurasia from 1979 to 2007, *IEEE Trans. Geosci. Remote Sens.*, *47*, 2996–3007.

Taylor, R. G., M. C. Todd, L. Kongola, L. Maurice, E. Nahozya, H. Sanga, and A. M. MacDonald (2013), Evidence of the dependence of groundwater resources on extreme rainfall in East Africa, *Nat. Clim. Change*, *3*, 374–378.

Taylor, S., X. Feng, M. Williams, and J. McNamara (2002), How isotopic fractionation of snowmelt affects hydrograph separation, *Hydrol. Processes*, *16*, 3683–3690.

Tweed, S. O., T. R. Weaver, and I. Cartwright (2005), Distinguishing groundwater flow paths in different fractured-rock aquifers using groundwater chemistry: Dandenong Ranges, southeast Australia, *Hydrogeol. J.*, *13*, 771–786.

Vachon, R. W., J. M. Welker, J. W. C. White, and B. H. Vaughn (2010), Monthly precipitation isoscapes (δ^{18}O) of the United States: Connections with surface temperatures, moisture source conditions, and air mass trajectories, *J. Geophys. Res.*, *115*, D21126, doi:10.1029/2010JD014105.

Van Beynen, P., and P. Febbroriello (2006), Seasonal isotopic variability of precipitation and cave drip water at Indian Oven Cave, New York, *Hydrol. Processes*, *20*, 1793–1803.

Vera, C., G. Silvestri, B. Liebmann, and P. González (2006), Climate change scenarios for seasonal precipitation in South America from IPCC-AR4 models, *Geophys. Res. Lett.*, *33*, L13707, doi:10.1029/2006GL025759.

Vogel, J. C., D. Ehhalt, and W. Roether (1963), A survey of the natural isotopes of water in South Africa, in *Proceedings of Tokyo Conference on Radioisotopes in Hydrology*, pp. 407–416, Int. At. Energy Agency, Vienna.

Voss, K. A., J. S. Famiglietti, M. Lo, C. Linage, M. Rodell, and S. C. Swenson (2013), Groundwater depletion in the Middle East from GRACE with implications for transboundary water management in the Tigris-Euphrates-Western Iran region, *Water Resour. Res.*, *49*, doi:10.1002/wrcr.20078.

Wada, Y., L. P. H. van Beek, C. M. van Kempen, J. W. T. M. Reckman, S. Vasek, and M. F. P. Bierkens (2010), Global depletion of groundwater resources, *Geophys. Res. Lett.*, *38*, L20402, doi:10.1029/2010GL044571.

Wada, Y., L. P. H. van Beek, and M. F. P. Bierkens (2012a), Nonsustainable groundwater sustaining irrigation: A global assessment, *Water Resour. Res.*, *48*, W00L06, doi:10.1029/2011WR010562.

Wada, Y., L. P. H. van Beek, F. C. S. Weiland, B. F. Chao, Y.-H. Wu, and M. F. P. Bierkens (2012b), Past and future contribution of global groundwater depletion to sea-level rise, *Geophys. Res. Lett.*, *39*, L09402, doi:10.1029/2012GL051230.

Wada, Y., D. Wisser, and M. F. P. Bierkens (2014), Global modeling of withdrawal, allocation and consumptive use of surface water and groundwater resources, *Earth Syst. Dyn.*, *5*, 15–40.

Wallick, E. I. (1981), Chemical evolution of groundwater in a drainage basin of Holocene age, east-central Alberta, Canada, *J. Hydrol.*, *54*, 245–283.

Walraevens, K., I. Vandecasteele, K. Martens, J. Nyssen, J. Moeyersons, T. Gebreyohannes, F. de Smedt, J. Poesen, J. Deckers, and M. Van Camp (2009), Groundwater recharge and flow in a small mountain catchment in northern Ethiopia, *Hydrol. Sci. J.*, *54*, 739–753.

Wang, L., F. Hu, L. Yin, L. Wan, and Q. Yu (2013), Hydrochemical and isotopic study of groundwater in the Yinchuan plain, China, *Environ. Earth Sci.*, *69*, 2037–2057.

Wanke, H., A. Dünkeloh, and P. Udluft (2008), Groundwater recharge assessment for the Kalahari catchment of north-eastern Namibia and north-western Botswana with a regional-scale water balance model, *Water Resour. Manage.*, *22*, 1143–1158.

Wassenaar, L. I., S. L. Van Wilgenburg, K. Larson, and K. A. Hobson (2009), A groundwater isoscape (δD, δ^{18}O) for Mexico, *J. Geochem. Explor.*, *102*, 123–136.

Welker, J. M. (2000), Isotopic (δ^{18}O) characteristics of weekly precipitation collected across the USA: An initial analysis with application to water source studies, *Hydrol. Processes*, *14*, 1449–1464.

Welker, J. M. (2012), ENSO effects on the isotopic (δ^{18}O, δ^{2}H and d-excess) of precipitation across the US using a long-term network (USNIP), *Rapid Commun. Mass Spectrom.*, *17*, 1655–1660.

Welker, J. M., S. McClelland, and T. W. Weaver (1991), Soil water retention after natural and simulated rainfall on a temperate grassland, *Theor. Appl. Climatol.*, *44*, 447–453.

Williams, J. W. (2003), Variations in tree cover in North America since the last glacial maximum, *Global Planet. Change*, *35*, 1–23.

Williams, P. W., and A. Fowler (2002), Relationship between oxygen isotopes in rainfall, cave percolation waters at Waitomo, New Zealand, *J. Hydrol.*, *41*, 53–70.

Winnick, M., J. M. Welker, and P. Chamberlain (2013), Stable Isotope evidence of El Nino like circulation in Pliocene western United States, *Clim. Past*, *9*, 903–912.

Winograd, I. J., T. B. Coplen, J. M. Landwehr, A. C. Riggs, K. R. Ludwig, B. J. Szabo, P. T. Kolesar, and K. M. Revesz (1992), Continuous 500,000-year climate record from vein calcite in Devils Hole, Nevada, *Science*, *258*, 255–260.

Winograd, I. J., A. C. Riggs, and T. B. Coplen (1998), The relative contributions of summer and cool-season precipitation to groundwater recharge, Spring Mountains, Nevada, USA, *Hydrogeol. J.*, *6*, 77–93.

Wischusen, J. D., L. K. Fifield, and R. G. Cresswell (2004), Hydrogeology of Palm Valley, central Australia: A Pleistocene flora refuge? *J. Hydrol.*, *293*, 20–46.

Yechieli, Y., U. Kafri, and O. Sivan (2009), The inter-relationship between coastal sub-aquifers and the Mediterranean Sea, deduced from radioactive isotopes analysis, *Hydrogeol. J.*, *17*, 265–274.

Yeh, P. J. F., and J. S. Famiglietti (2009), Regional groundwater evapotranspiration in Illinois, *J. Hydrometeorol.*, *10*, 464–478.

Yonge, C. J., D. C. Ford, J. Gray, and H. P. Schwarcz (1985), Stable isotope studies of cave seepage water, *Chem. Geol. Isot. Geosci. Sec.*, *58*, 97–105.

Yoshimura, K., T. Oki, N. Ohte, and S. Kanae (2003), A quantitative analysis of short-term ^{18}O variability with a Rayleigh-type isotope circulation model, *J. Geophys. Res.*, *108*(D20), 4647, doi:10.1029/2003JD003477.

Zuber, A., S. M. Weise, J. Motyka, Osenbrück, K., and K. Różański (2004), Age and flow pattern of groundwater in a Jurassic limestone aquifer and related Tertiary sands derived from combined isotope, noble gas and chemical data, *J. Hydrol.*, *286*, 87–112.

